VIROLOGY

A universal influenza mRNA vaccine candidate boosts T cell responses and reduces zoonotic influenza virus disease in ferrets

Koen van de Ven[1], Josien Lanfermeijer[1,2], Harry van Dijken[1], Hiromi Muramatsu[3], Caroline Vilas Boas de Melo[1], Stefanie Lenz[1], Florence Peters[1], Mitchell B. Beattie[4], Paulo J. C. Lin[4], José A. Ferreira[5], Judith van den Brand[6], Debbie van Baarle[1,7], Norbert Pardi[3]*, Jørgen de Jonge[1]*

Universal influenza vaccines should protect against continuously evolving and newly emerging influenza viruses. T cells may be an essential target of such vaccines, as they can clear infected cells through recognition of conserved influenza virus epitopes. We evaluated a novel T cell–inducing nucleoside-modified messenger RNA (mRNA) vaccine that encodes the conserved nucleoprotein, matrix protein 1, and polymerase basic protein 1 of an H1N1 influenza virus. To mimic the human situation, we applied the mRNA vaccine as a prime-boost regimen in naïve ferrets (mimicking young children) and as a booster in influenza-experienced ferrets (mimicking adults). The vaccine induced and boosted broadly reactive T cells in the circulation, bone marrow, and respiratory tract. Booster vaccination enhanced protection against heterosubtypic infection with a potential pandemic H7N9 influenza virus in influenza-experienced ferrets. Our findings show that mRNA vaccines encoding internal influenza virus proteins represent a promising strategy to induce broadly protective T cell immunity against influenza viruses.

INTRODUCTION

Influenza viruses infect 5 to 15% of the world population annually, resulting in approximately 290 to 650 thousands of deaths worldwide (*1*, *2*). While vaccines mitigate influenza virus–induced morbidity and mortality, the effectiveness of inactivated influenza virus vaccines is insufficient (*3*, *4*). These vaccines mainly induce strain-specific immunity and are therefore limited in their ability to protect against mutated or newly introduced influenza virus strains. Animal-to-human transmissions of influenza A viruses pose a particular risk, as seasonal influenza vaccination does not offer protection against these strains. There are ample examples of influenza viruses crossing the species barrier and causing a pandemic, with the Spanish flu of 1918 as the most marked known example (*5*, *6*). Recent zoonotic transmissions of highly pathogenic avian influenza viruses, such as H5N1 and H7N9, have occurred frequently and are associated with high mortality rates (*7*, *8*). Especially alarming is the recent rise in outbreaks of these viruses in poultry farms and among migratory birds in Europe and other parts of the world (*9*). Although human-to-human transmission of these viruses has been limited so far, experimental work indicates that only few mutations are required to enhance transmission among humans, highlighting their pandemic potential (*10*–*12*). This emphasizes the ongoing threat posed by influenza viruses and the requirement for a broadly reactive influenza vaccine that protects against all influenza subtypes.

The narrow protection of inactivated influenza virus vaccines is mainly due to the induction of strain-specific antibodies against the highly variable globular head domain of influenza virus hemagglutinin (HA) (*13*). New vaccine concepts strive to provide a wider range of protection by inducing responses against more conserved protein domains (*14*). One way to achieve this is by inducing T cell responses, as T cells can recognize epitopes derived from conserved influenza virus proteins such as nucleoprotein (NP), matrix protein 1 (M1), and polymerase basic protein 1 (PB1) (*15*–*17*). T cells can clear infected cells, and T cell immunity is associated with improved influenza disease outcome in humans (*18*–*22*). In addition, animal models have confirmed that T cells can protect against heterosubtypic influenza virus infections (*23*–*29*). For these reasons, various new influenza vaccine concepts focus on inducing protective T cell immunity (*13*, *29*, *30*).

In recent years, lipid nanoparticle (LNP)–encapsulated nucleoside-modified mRNA (mRNA-LNP) has shown to be a potent novel vaccine format against influenza and other infectious diseases (*31*, *32*). The potency of the mRNA-LNP platform has been demonstrated by the rapid development and successful worldwide use of nucleoside-modified mRNA-LNP–based SARS-CoV-2 (severe acute respiratory syndrome coronavirus 2) vaccines (*33*). mRNA-LNP induces both T cell and antibody responses (*34*–*38*) and is therefore a promising platform for improvedinfluenza vaccines. In addition, mRNA-LNP vaccines can be rapidly produced and are easily adjusted to new emerging viral variants (*39*). Multiple influenza vaccines based on mRNA-LNP are currently in development, with promising early results (*40*–*44*). These vaccines, however, primarily focus on inducing humoral responses, without fully using the potential of T cell immunity against conserved internal influenza proteins.

[1]Centre for Infectious Disease Control, National Institute for Public Health and the Environment (RIVM), Bilthoven, Netherlands. [2]Center for Translational Immunology, University Medical Center Utrecht, Utrecht, Netherlands. [3]Department of Microbiology, Perelman School of Medicine, University of Pennsylvania, Philadelphia, PA, USA. [4]Acuitas Therapeutics, Vancouver, BC V6T 1Z3, Canada. [5]Department of Statistics, Informatics and Modelling, National Institute for Public Health and the Environment (RIVM), Bilthoven, Netherlands. [6]Division of Pathology, Faculty of Veterinary Medicine, Utrecht University, Utrecht, Netherlands. [7]Department of Medical Microbiology and Infection Prevention, Virology and Immunology Research Group, University Medical Center Groningen, Groningen, Netherlands.
*Corresponding author. Email: pnorbert@pennmedicine.upenn.edu (N.P.); jorgen.de.jonge@rivm.nl (J.d.J.)

There is still very limited information about the potential of mRNA-LNP vaccines for inducing broadly protective T cell responses against influenza virus infections. We set out to remedy this knowledge gap by evaluating the immunogenicity and protective efficacy of a novel mRNA-LNP influenza vaccine in a highly relevant ferret model. We have previously shown in ferrets that circulating and respiratory T cells recognize conserved influenza virus epitopes and can protect against heterosubtypic influenza virus infection (*24*). Here, we investigated whether we could induce and enhance this protective immunity by vaccination with nucleoside-modified mRNA-LNP encoding three conserved internal proteins of H1N1 influenza virus, NP, M1, and PB1 (mRNA-Flu). To mimic the human situation, which consists of both naïve young children and influenza-experienced individuals, we evaluated mRNA-Flu as a prime-boost regimen in naïve ferrets (a model for naïve children) and as a booster in influenza-experienced ferrets (a model for influenza-experienced individuals). Both strategies successfully induced and boosted systemic and respiratory T cell responses, but mRNA-Flu vaccination in influenza-experienced ferrets resulted in higher and broader responses. Moreover, mRNA-Flu booster immunization reduced disease severity in influenza-experienced ferrets after challenge with a potential pandemic avian H7N9 influenza virus, whereas mock-boosted influenza-experienced ferrets were not protected. Our results demonstrate that broadly reactive T cell immunity is boosted by a nucleoside-modified mRNA-LNP vaccine that encodes several internal influenza virus proteins. This mRNA-LNP vaccine enhanced protection against heterosubtypic influenza virus infection and is a promising strategy for the development of a universal influenza vaccine.

RESULTS

Cell transfection studies

We designed the mRNA vaccine based on the NP, M1, and PB1 proteins of the A/Michigan/45/2015 H1N1 pandemic influenza virus because these proteins are highly conserved among antigenically distant influenza virus strains (table S1) and they have been shown to be immunogenic in humans (*24*, *45*). Before the vaccination experiments, we confirmed protein production from each antigen-encoding mRNA in cell transfection studies. Human embryonic kidney (HEK) 293T cells were transfected with M1-, PB1-, or control firefly luciferase-encoding mRNAs, and protein production from the M1 and PB1 constructs was confirmed by Western blotting (fig. S1). The NP-encoding mRNA was validated in an earlier publication (*40*).

Study setup

To model mRNA-Flu vaccination in both naïve and influenza-experienced humans, we followed a prime-boost strategy with different regimens (Fig. 1A). Naïve ferrets were prime-boosted with mRNA-Flu on days 0 and 42, modeling naïve individuals (group mRNA/mRNA, $n = 14$). The vaccine was administered intramuscularly and contained 50 μg of NP, M1, and PB1 mRNA-LNP (the total mRNA dose was 150 μg). Another group of ferrets was primed on day 0 by intranasal infection with 10^6 median tissue culture infectious dose ($TCID_{50}$) A/California/07/2009 (H1N1) influenza virus, followed by booster vaccination with mRNA-Flu on day 42 to mimic vaccination of influenza virus–experienced individuals (group H1N1/mRNA, $n = 14$). As a control for this treatment, another group of ferrets received the same priming (H1N1 infection) but a mock booster with mRNA-LNP encoding firefly luciferase (group H1N1/mock, $n = 14$) on day 42. A placebo group that received only phosphate-buffered saline (PBS) as a prime boost served as a negative control ($n = 14$). The positive control consisted of ferrets that were primed by H1N1 infection and boosted with 10^6 $TCID_{50}$ A/Uruguay/217/2007 (H3N2) influenza virus, as a secondary heterosubtypic influenza infection as it is a very potent booster of T cell responses (group H1N1/H3N2, $n = 7$) (*24*). Blood was collected at 0, 14, 42, 56, and 70 days post priming (dpp). Four weeks after the booster (70 dpp), ferrets were euthanized, and systemic and local T cell responses were studied.

The mRNA-based T cell vaccine induces and boosts systemic cellular responses against conserved influenza virus proteins

We evaluated the cellular responses induced by mRNA-Flu vaccination by stimulation of peripheral blood mononuclear cells (PBMCs) from immunized ferrets with overlapping peptide pools of H1N1 NP, M1, and PB1 in interferon-γ (IFN-γ) enzyme-linked immunospot (ELISpot) assays. A single dose of mRNA-Flu induced cellular responses against NP but not to M1 and PB1 at 14 dpp (Fig. 1B and fig. S2A). The responses were stronger and broader in H1N1 influenza virus–primed ferrets as they displayed responses against NP, M1, and PB1. The cellular response against NP in mRNA-primed ferrets increased further between 14 and 42 dpp, while this response was already contracting in H1N1-primed ferrets. This might be due to the long availability of influenza antigens produced from the mRNA-LNP vaccines after intramuscular immunization (*46*).

mRNA-Flu vaccination at 42 dpp boosted existing cellular responses, irrespective of whether ferrets were initially primed with mRNA-Flu or H1N1 influenza (Fig. 1B). At 56 and 70 dpp, NP-specific responses were similar between mRNA/mRNA and H1N1/mRNA ferrets. The responses against M1 and PB1 were still weaker in the mRNA/mRNA group, although they were clearly boosted as approximately half of the animals developed cellular responses after the second vaccination (Fig. 1B and fig. S2B). NP-specific cellular responses in mRNA/mRNA and H1N1/mRNA ferrets were similarly robust to that measured in H1N1-experienced ferrets boosted with H3N2 influenza virus infection. This finding indicates that nucleoside-modified mRNA-LNP vaccination can be as effective in boosting existing T cell responses as a heterosubtypic influenza virus infection.

Because of the high level of conservation of internal influenza virus proteins even among different influenza subtypes (>90%; table S1), T cells induced by mRNA-Flu or H1N1-priming should be reactive to a wide range of influenza viruses. Cellular responses measured in PBMCs after stimulation with H1N1 peptide pools correlated strongly with responses obtained with peptide pools specific for an H2N2 influenza virus (A/Leningrad/134/17/57; fig. S2C). Live virus stimulations confirmed these findings as we observed substantial responses against heterosubtypic influenza viruses H3N2, H5N1 (A/Vietnam/1204/2004), and H7N9 (A/Anhui/1/2013; Fig. 1C and fig. S2D). In conclusion, immunization with mRNA-Flu induces and boosts the cellular response that is cross-reactive with a wide range of influenza viruses due to targeting conserved influenza virus epitopes.

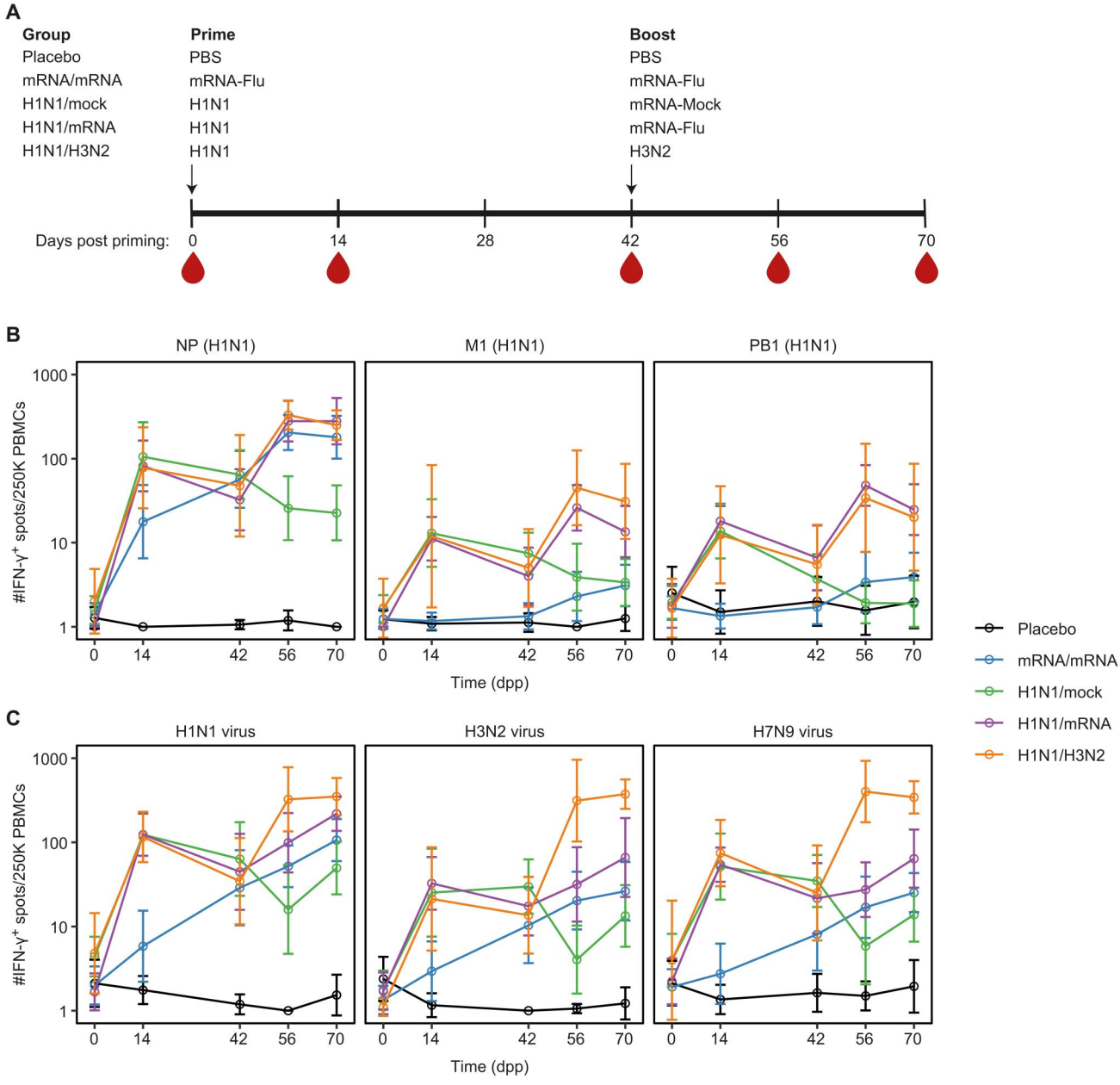

Fig. 1. Cellular responses in blood after prime-boost immunization with mRNA-Flu. (**A**) Study layout depicting the prime-boost strategy. On day 0, ferrets were primed intranasally with PBS and 10^6 $TCID_{50}$ H1N1 influenza virus (A/California/07/2009) or primed intramuscularly with mRNA-LNPs encoding for NP, M1, and PB1 (50 μg per mRNA-LNP; mRNA-Flu). Ferrets primed with PBS (group placebo) or mRNA-Flu (group mRNA/mRNA) received the same treatment as booster 42 dpp. H1N1-primed ferrets were boosted intramuscularly with mRNA-Flu (H1N1/mRNA-Flu) and mRNA-LNP encoding firefly luciferase (50 μg; H1N1/mock) or boosted intranasally with 10^6 $TCID_{50}$ H3N2 influenza virus (H1N1/H3N2; A/Uruguay/217/2007). Blood was collected on 0, 14, 42, 56, and 70 dpp. Ferrets were euthanized 70 dpp to study cellular responses in tissues. (**B** and **C**) Cellular responses measured by interferon-γ (IFN-γ) ELISpot after 20-hour stimulation of peripheral blood mononuclear cells (PBMCs) with (B) H1N1 NP, M1, and PB1 overlapping peptide pools or (C) live influenza viruses H1N1, H3N2, or H7N9 (A/Anhui/1/2013). Data were corrected for medium background and are visualized as geometric mean + geometric SD. $n = 7$ for H1N1/H3N2 and $n = 12$ to 14 for all other groups. Statistics are detailed in data file S1.

The mRNA-based T cell vaccine induces and boosts cellular responses in the respiratory tract and bone marrow

T cells located in the respiratory tract are essential for protection against heterosubtypic influenza virus infections (*27*, *47*). To determine whether mRNA-Flu vaccination is also able to induce and boost T cell responses in the respiratory tract, we assessed cellular immune responses in the bronchoalveolar lavage (BAL) fluid and nasal turbinates (NTs) of immunized ferrets by IFN-γ ELISpot at 70 dpp. Despite intramuscular vaccine administration, mRNA-Flu induced robust cellular responses against NP in the NT but not in the BAL fluid of mRNA/mRNA ferrets (Fig. 2A and fig. S2D). The effect of mRNA-Flu vaccination was even more potent in H1N1-primed ferrets. Vaccination effectively increased NP-, M1-, and PB1-specific T cell responses in the NT of H1N1/mRNA ferrets

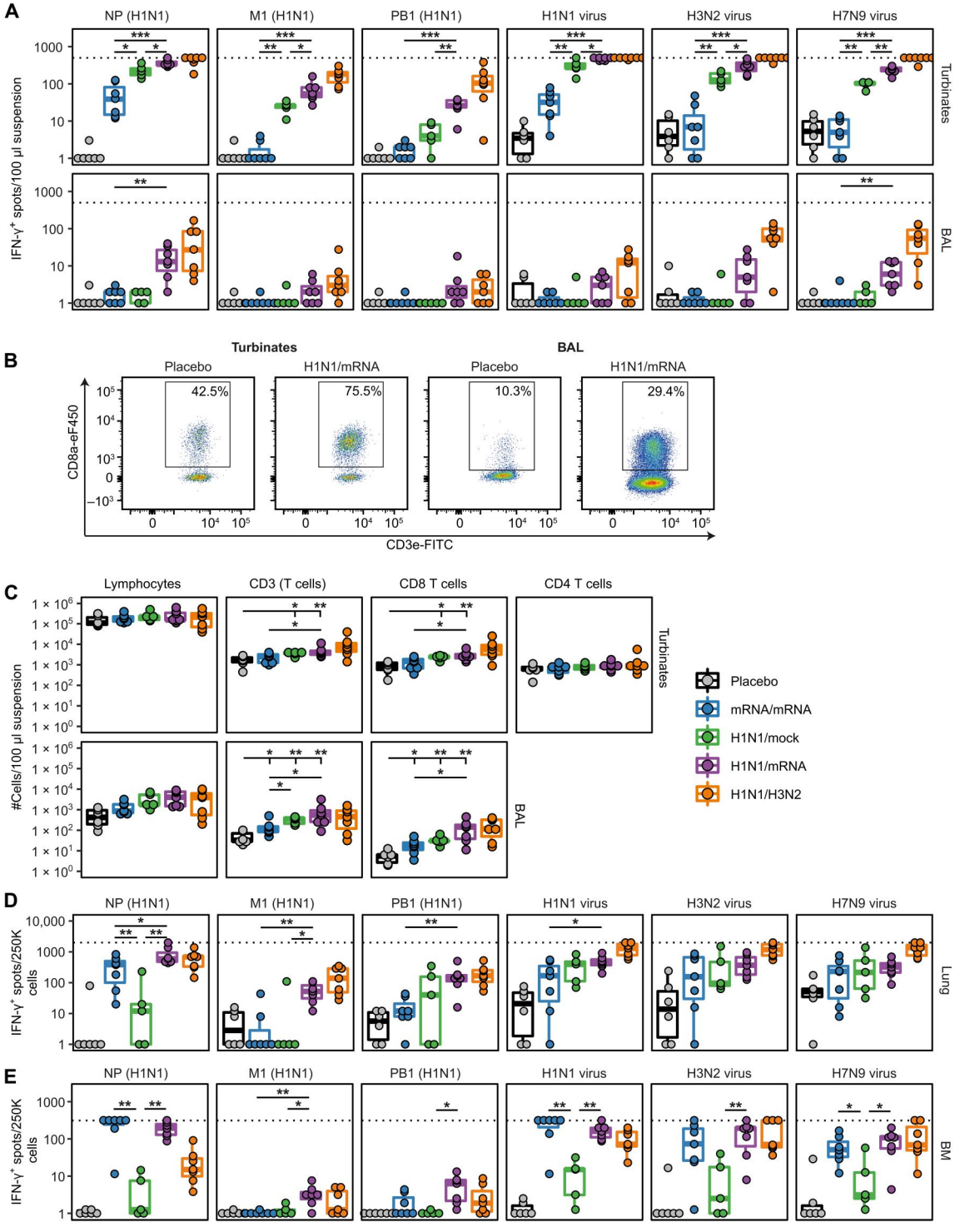

Fig. 2. Cellular responses in respiratory compartments and BM of immunized ferrets. (**A**) Cellular responses measured by IFN-γ ELISpot after 20-hour stimulation with overlapping H1N1 peptide pools or live influenza virus using cells derived from NTs and BAL fluid. (**B** and **C**) Cell counts in NTs and BAL as measured by flow cytometry. (B) Flow cytometry plot displaying the $CD8^+$ T cell population in representative turbinate and BAL samples. (C) Counts of different cell populations per 100 µl of cell suspension. $CD4^+$ T cell counts are not displayed for BAL, as the α-CD4–APC staining was not consistent between BAL samples. (**D** and **E**) Cellular responses measured by IFN-γ ELISpot after 20-hour stimulation with overlapping H1N1 peptide pools or live influenza virus of cells derived from (D) lung or (E) BM. ELISpot data were corrected for medium background. Box plots depict the median and 25 and 75% percentiles, where the top and bottom whiskers extend to the smallest and largest value, respectively, within 1.5 × the interquartile ranges. (A and C to E) Each dot represents one animal and $n = 5$ to 7. For visualization purposes, only comparisons between groups mRNA/mRNA, H1N1/mock, and H1N1/mRNA are shown. (C) Comparisons with placebo ferrets are additionally shown. An overview of all statistical comparisons is shown in data file S1. $^*P < 0.05$, $^{**}P < 0.01$, and $^{***}P < 0.001$.

relative to H1N1/mock and mRNA/mRNA ferrets. NP-specific responses in the BAL fluid of H1N1/mRNA ferrets also demonstrated an increase compared to H1N1/mock ferrets. Responses against homologous (H1N1) and heterosubtypic (H3N2, H5N1, and H7N9) influenza viruses were also higher in the NT (significant) and BAL (trend) of H1N1/mRNA ferrets compared to mRNA/mRNA and H1N1/mock ferrets. All groups that were initially primed intranasally with H1N1 influenza virus displayed stronger cellular responses in the NT than the mRNA/mRNA group, irrespective of whether they received a booster, suggesting that the site of priming dictates the response.

To determine whether mRNA-Flu vaccination also increased absolute T cell numbers in the respiratory tract, we measured cell counts in the NT and BAL by flow cytometry. Compared to placebo ferrets, T cell counts ($CD3^+$) in the NT were only significantly increased in H1N1/mRNA and H1N1/H3N2 ferrets (Fig. 2, B and C, and fig. S3). This was primarily due to an increase in $CD8^+$ T cells because $CD4^+$ T cell counts did not significantly differ in the placebo animals. In BAL, mRNA/mRNA treatment enhanced both $CD3^+$ and $CD8^+$ T cell counts compared to placebo ferrets. The effect of prime boost with mRNA-Flu vaccination on T cell numbers in the BAL was less effective compared to a single influenza virus infection, as H1N1/mock-treated ferrets displayed higher $CD3^+$ numbers compared to mRNA/mRNA ferrets. To determine whether the increased T cell counts correlated with increased IFN-γ responses, we performed a correlation analysis between population counts and IFN-γ–ELISpot counts induced by H1N1 peptide pool stimulation. $CD8^+$ T cell counts showed the strongest correlation with IFN-γ–ELISpot responses, indicating that the IFN-γ response in the BAL and NT was mainly mediated by $CD8^+$ T cells (fig. S4).

We additionally investigated cellular responses by IFN-γ ELISpot in the lungs that were perfused with a saline solution to reduce contamination of lung-derived lymphocytes with circulating lymphocytes. We observed robust cellular responses against NP but not to M1 and PB1 in the lungs of mRNA/mRNA ferrets (Fig. 2D). Responses in the lung of mRNA/mRNA ferrets exceeded those measured in the blood, indicating that it is unlikely that the increase is due to contamination with circulating lymphocytes. In H1N1 influenza virus-primed ferrets, mRNA-Flu vaccination significantly boosted cellular responses against NP and M1 in the lung (group H1N1/mRNA versus H1N1/mock) to similar levels that were achieved by a secondary natural infection with influenza virus (group H1N1/H3N2). Cellular responses to heterosubtypic virus stimulations (H3N2, H7N9, and H5N1) were however similar between the H1N1/mRNA and mRNA/mRNA groups, indicating that mRNA/mRNA ferrets were not severely hampered by the low responses against M1 and PB1 (Fig. 2D and fig. S2D).

Next, we investigated the presence of T cell responses in the bone marrow (BM) because it is a reservoir for memory T cells (*48*). mRNA/mRNA treatment induced strong T cell responses against NP in the BM (Fig. 2E and fig. S2D). Responses were similarly robust in H1N1/mRNA ferrets, while they were modest in H1N1/mock and H1N1/H3N2 ferrets. M1 and PB1 peptide pool responses were low for all groups in the BM, although these responses were present in other tissues (fig. S5). The response to homologous (H1N1) and heterosubtypic [H3N2 (not significant for mRNA/mRNA), H5N1, and H7N9] influenza viruses was increased in both the mRNA/mRNA and H1N1/mRNA groups compared to H1N1/mock ferrets (Fig. 2E and fig. S2D). Together, these findings clearly demonstrate that the nucleoside-modified mRNA-LNP influenza T cell vaccine is able to boost influenza virus–specific T cell responses in the blood, respiratory tract, and BM. Overall, compared to mRNA/mRNA ferrets, cellular responses were broader in H1N1/mRNA ferrets because they displayed robust M1- and PB1-specific responses in addition to NP-induced immunity (fig. S5).

The mRNA-based T cell vaccine induces and boosts both $CD4^+$ and $CD8^+$ T cell responses in PBMCs, spleen, lung, and BM

To study the T cell response in more detail, we measured IFN-γ production of $CD4^+$ and $CD8^+$ T cells at 70 dpp by flow cytometric analysis. We stimulated lymphocytes derived from blood, spleen, lung, and BM with an H1N1 peptide cocktail consisting of NP, M1, and PB1 peptide pools. mRNA/mRNA and H1N1/mRNA ferrets had significantly more $CD8^+IFN\text{-}\gamma^+$ T cells in all tissues investigated relative to the placebo and H1N1/mock animals (Fig. 3, A and B, and fig. S6, A and B). In PBMC and lung, H1N1/mRNA ferrets demonstrated significantly stronger $CD8^+$ T cell responses compared to mRNA/mRNA ferrets. The opposite was observed in the BM where mRNA/mRNA ferrets showed the most robust IFN-γ response, although this was not significantly stronger compared to H1N1/mRNA ferrets. The H1N1 peptide cocktail–induced IFN-γ responses in PBMCs, spleen, and BM of H1N1/mRNA ferrets even exceeded those measured in ferrets boosted by a secondary infection (H1N1/H3N2 ferrets), further demonstrating the potency of the mRNA-Flu vaccine. In comparison to $CD8^+$ T cells, $CD4^+$ T cell responses were weaker in most cases, and differences between groups were slightly smaller (Fig. 3, A and C, and fig. S6, A and C). Still, mRNA-Flu vaccination induced $CD4^+$ T cell responses in all investigated compartments of mRNA/mRNA ferrets and significantly boosted $CD4^+$ T cell responses in the blood and BM of H1N1/mRNA ferrets compared to H1N1/mock ferrets.

Stimulations with live H1N1 or H3N2 influenza virus yielded similar results to those obtained with H1N1 peptide cocktail stimulations (Fig. 3D). However, there was a trend that $CD8^+$ T cell responses in lungs of H1N1/H3N2 ferrets were slightly stronger than in H1N1/mRNA ferrets. This might be due to T cells that recognize conserved epitopes in proteins other than NP, M1, and PB1. $CD4^+$ T cell responses after virus stimulation were comparable to their $CD8^+$ T cell counterparts, although $CD4^+$ T cell responses in the lungs could not be interpreted because of high IFN-γ background responses in placebo animals (fig. S6D). Stimulations with H3N2 virus resulted in weaker $CD4^+$ and $CD8^+$ T cell responses compared to H1N1 virus stimulations (Fig. 3D and fig. S6D), which was not observed in the IFN-γ ELISpot assays (Fig. 2). This is likely due to a lower virus-to-cell ratio used for H3N2 stimulation in flow cytometry assays.

To investigate whether mRNA-Flu vaccination leads to skewing of the T cell response toward a $CD4^+$ or $CD8^+$ T cell phenotype, we calculated the $CD8^+/CD4^+$ ratio within the $CD3^+IFN\text{-}\gamma^+$ population after H1N1 peptide cocktail or H1N1 virus stimulation. In the tissues investigated, H1N1/mock and H1N1/H3N2 ferrets tended to have an average ratio of 1, demonstrating that IFN-γ responses were approximately evenly distributed between $CD4^+$ and $CD8^+$ T cells (Fig. 3E and fig. S6E). In all tissues, there was a clear skewing toward a $CD8^+$ T cell response in groups that received mRNA-Flu vaccination. Given the robust $CD4^+$ T cell responses in mRNA-Flu–immunized ferrets, skewing toward a $CD8^+$ T cell

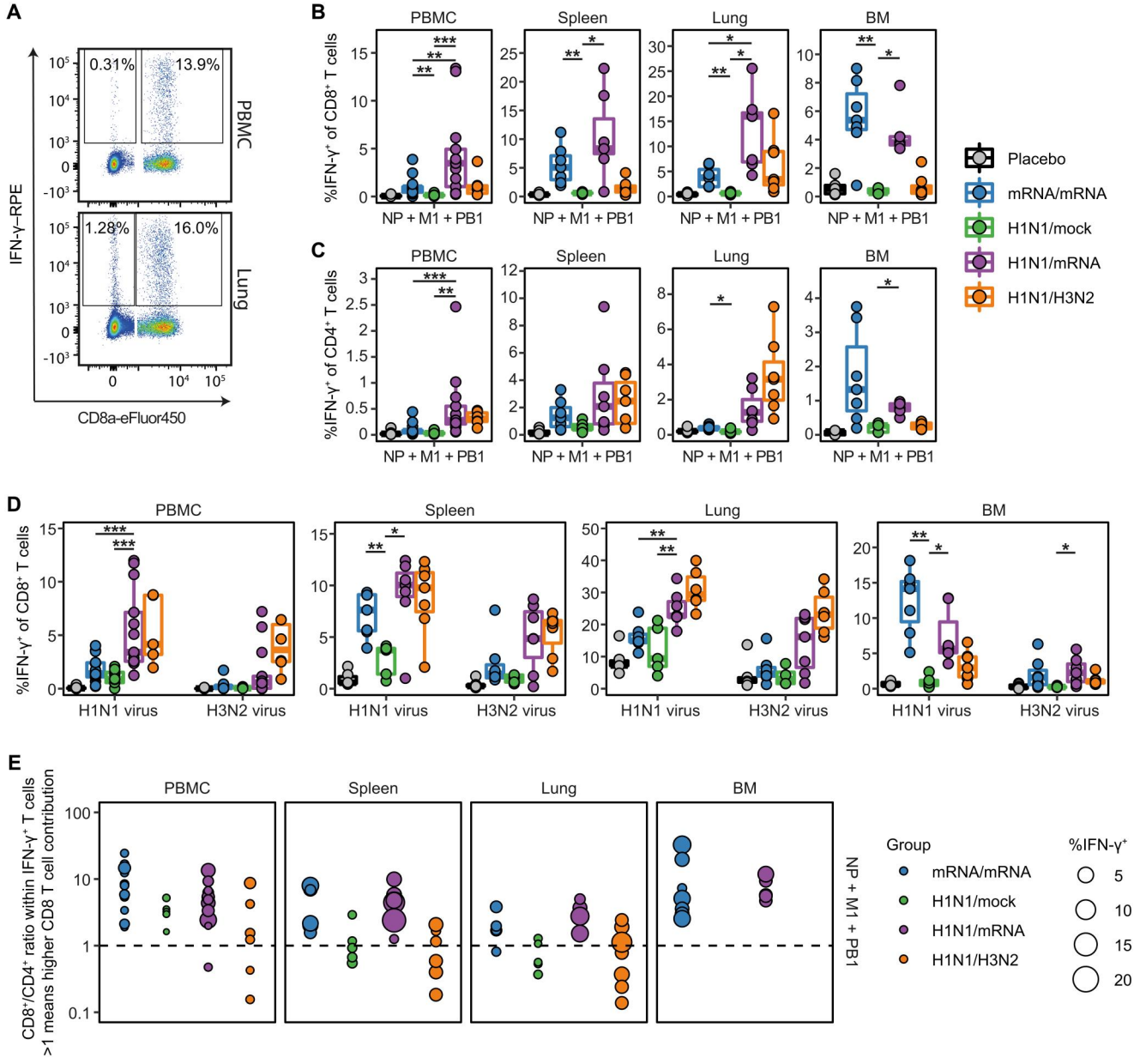

Fig. 3. IFN-γ responses of CD4⁺ and CD8⁺ T cells in PBMCs, spleen, lung, and BM of immunized ferrets. Lymphocytes were stimulated with a peptide cocktail containing H1N1 NP, M1, and PB1 peptide pools or live influenza virus. Cells were stained for intracellular IFN-γ and analyzed by flow cytometry. (**A**) Flow cytometry plots depict representative CD4⁺ and CD8⁺ T cell responses of H1N1/mRNA-treated ferrets after peptide cocktail stimulation. Numbers indicate percentage of CD4⁺ (left quadrant) and CD8⁺ (right quadrant) T cells expressing IFN-γ. (**B** and **C**) Percentage IFN-γ⁺ cells within CD8⁺ (B) and CD4⁺ (C) T cell populations after peptide cocktail stimulation. (**D**) Percentage IFN-γ⁺ cells within CD8⁺ T cell population after stimulation with H1N1 (A/California/07/2009) or H3N2 (A/Uruguay/217/2007) influenza viruses. (**E**) Ratio between CD8⁺ and CD4⁺ T cells within the CD3⁺ IFN-γ⁺ T cell population after peptide cocktail stimulation. Dotted line represents a ratio of 1, and samples with less than 50 CD3⁺ IFN-γ⁺ cells were excluded from the analysis. Each dot represents one ferret, and the dot size is relative to the total IFN-γ response (%IFN-γ⁺ of CD4⁺ and CD8⁺ T cells). Box plots depict the median and 25 and 75% percentiles, where the top and bottom whiskers extend to the smallest and largest value, respectively, within 1.5 × the interquartile ranges. (B to E) Each dot represents one animal. $n = 4$ to 13 for PBMC and $n = 4$ to 7 for lung, spleen, and BM. For visualization purposes, only comparisons between groups mRNA/mRNA, H1N1/mock, and H1N1/mRNA are shown. No statistics were performed for (E). An overview of all statistical comparisons is shown in data file S1. *$P < 0.05$, **$P < 0.01$, and ***$P < 0.001$.

response is not caused by a low $CD4^+$ T cell response but by a very strong boosting of the $CD8^+$ T cell response. mRNA-Flu is thus a potent booster of both $CD4^+$ and $CD8^+$ T cell immunity.

H7N9 influenza disease is reduced in influenza virus–experienced ferrets after booster mRNA-Flu vaccination

Next, we investigated whether mRNA-Flu vaccination could protect against severe disease caused by a heterosubtypic avian influenza virus infection. We immunized ferrets as described above with the exception of H1N1/H3N2 ferrets and challenged these animals intratracheally with a lethal dose of 10^6 $TCID_{50}$ H7N9 influenza virus 4 weeks after the booster vaccination (Fig. 4A). At this time, the boosted T cell response is expected to be in its memory phase, similar to when (vaccinated) individuals are infected with influenza virus. Ferrets were euthanized 5 days post infection (dpi) to study viral replication and pathology.

mRNA-Flu vaccination enhanced protection against H7N9 disease in H1N1-primed ferrets. Weight loss of H1N1/mRNA ferrets was limited to 7% and stabilized 5 dpi, while placebo animals lost more than 17% of bodyweight on average and were still losing weight at 5 dpi (Fig. 4B). mRNA/mRNA ferrets showed mixed results, with weight loss in isolator 1 being similar to placebo (~15%) but less severe in isolator 2 (~11%). Notably, one (of six) placebo ferrets and three (of six) mRNA/mRNA ferrets displayed inactivity and severe impaired breathing at 4 dpi and needed to be euthanized because the human end points were reached. The mRNA/mRNA group was affected by a cage effect of unknown origin, as all ferrets that reached the humane end points were housed in one of the two isolators. The cage effect could not be explained by preexisting immunity or infection history with other viruses (e.g., influenza virus, Aleutian disease, and ferret corona viruses), as these were similar between groups (fig. S7 and table S2). The two mRNA/mRNA groups are therefore analyzed together but visualized separately. No cage effect was present in other treatment groups.

Weight data were in line with clinical symptoms, as H1N1/mRNA-treated ferrets had less difficulty with breathing and were more active compared to other groups at 4 and 5 dpi (Fig. 4C). The height and duration of fever were not influenced by prior treatment, as all groups displayed similar increases in body temperature (Fig. 4D and fig. S8A). Three animals in the mRNA/mRNA group showed hypothermia starting from 2 dpi and were euthanized at 4 dpi. Viral titers in nose and throat swabs were similar between groups at 2 and 3 dpi (Fig. 4E). By 5 dpi, however, viral titers were lower in both H1N1/mRNA and H1N1/mock ferrets when compared to placebo. mRNA/mRNA ferrets gave mixed results. While viral titers in the nose were similar to placebo at all time points investigated, viral titers in the throat at 5 dpi were significantly lower in surviving mRNA/mRNA ferrets compared to all other groups. We additionally measured viral titers in the lung tissue. Differences were small, but H1N1/mRNA ferrets displayed significantly lower viral titers compared to all other groups (Fig. 4F). Viral titers in the trachea were low for all groups, except for the placebo group, indicating that all strategies limited viral replication to some extent.

Despite the reduced disease severity in H1N1/mRNA ferrets, the lungs showed moderate to severe bronchointerstitial pneumonia, often related to the bronchioles and bronchi that extended to the alveoli, irrespective of treatment (Fig. 4G and fig. S8B). However, alveolar edema, hyperplasia of type II pneumocytes, and alveolar damage were somewhat reduced in H1N1/mRNA-vaccinated ferrets. We measured lung weight at 5 dpi as an independent measurement of lung pathology and found that H1N1/mRNA ferrets had significantly lower lung weights (Fig. 4H). This indicates that inflammation and the infection-induced lung edema were less severe, which is in line with the less impaired breathing that we observed in H1N1/mRNA ferrets. From these results, we conclude that nucleoside-modified mRNA-LNP influenza booster vaccination in H1N1-experienced ferrets was able to reduce H7N9 disease severity and virus replication.

Protection against H7N9 influenza virus is likely mediated by cellular responses

To assess whether enhanced cellular responses during H7N9 influenza virus infection are related to the observed disease outcomes, we collected PBMCs at 4 or 5 dpi (depending on when ferrets were euthanized) and stimulated cells with H1N1 peptide pools in an IFN-γ ELISpot assay. Although cellular responses against M1 and PB1 were low before infection (Fig. 1B), they became more substantial after infection (fig. S9), suggesting that M1- and PB1-specific T cells may play a role in the observed reduction in H7N9 disease parameters. Differences between groups were difficult to quantify because of the strong responses observed, which reached the upper limit of detection of the IFN-γ ELISpot assay.

To exclude the possibility that antibodies against H7N9 influenza virus played a role in the protection against H7N9 virus infection, we measured the level of antibodies in ferret sera before infection (70 dpp). We did not detect H7N9 virus–specific antibodies by hemagglutination inhibition (HI) and virus neutralization (VN) assays (Fig. 5, A and B). We additionally measured antibodies against H7N9 HA (H7), NP, and M1 proteins by enzyme-linked immunosorbent assay (ELISA), as not all influenza virus–specific antibodies can be detected by HI and VN assays. We did not find significant responses to H7, but we measured high antibody titers against NP and M1 (Fig. 5C). We could not investigate PB1-specific antibodies as no recombinant H7N9 influenza virus PB1 protein was commercially available. These findings indicate that HA-specific antibodies did not play a role in the disease reduction that we observed, but the role of NP-, M1-, and possibly PB1-specific antibodies remains to be investigated.

DISCUSSION

The coronavirus disease 2019 (COVID-19) pandemic has shown the enormous potential of the nucleoside-modified mRNA-LNP vaccine platform for inducing protective immune responses against SARS-CoV-2 infection in humans. This success is driving the development of mRNA-LNP vaccines against other pathogens, with influenza virus as a prime example. There are currently multiple mRNA-based influenza vaccines in the clinical phase of development (*49*). Most of these vaccines are designed to primarily induce neutralizing antibodies against the globular head domain of HA, which does not solve the problem of strain-specific immunity mediated by such antibodies. T cells could target a wider range of influenza viruses, but little is known about the potential of mRNA-LNP vaccines to induce protective influenza virus–specific T cell immunity. Here, we used a unique ferret model in which we could measure systemic and respiratory T cell responses to evaluate

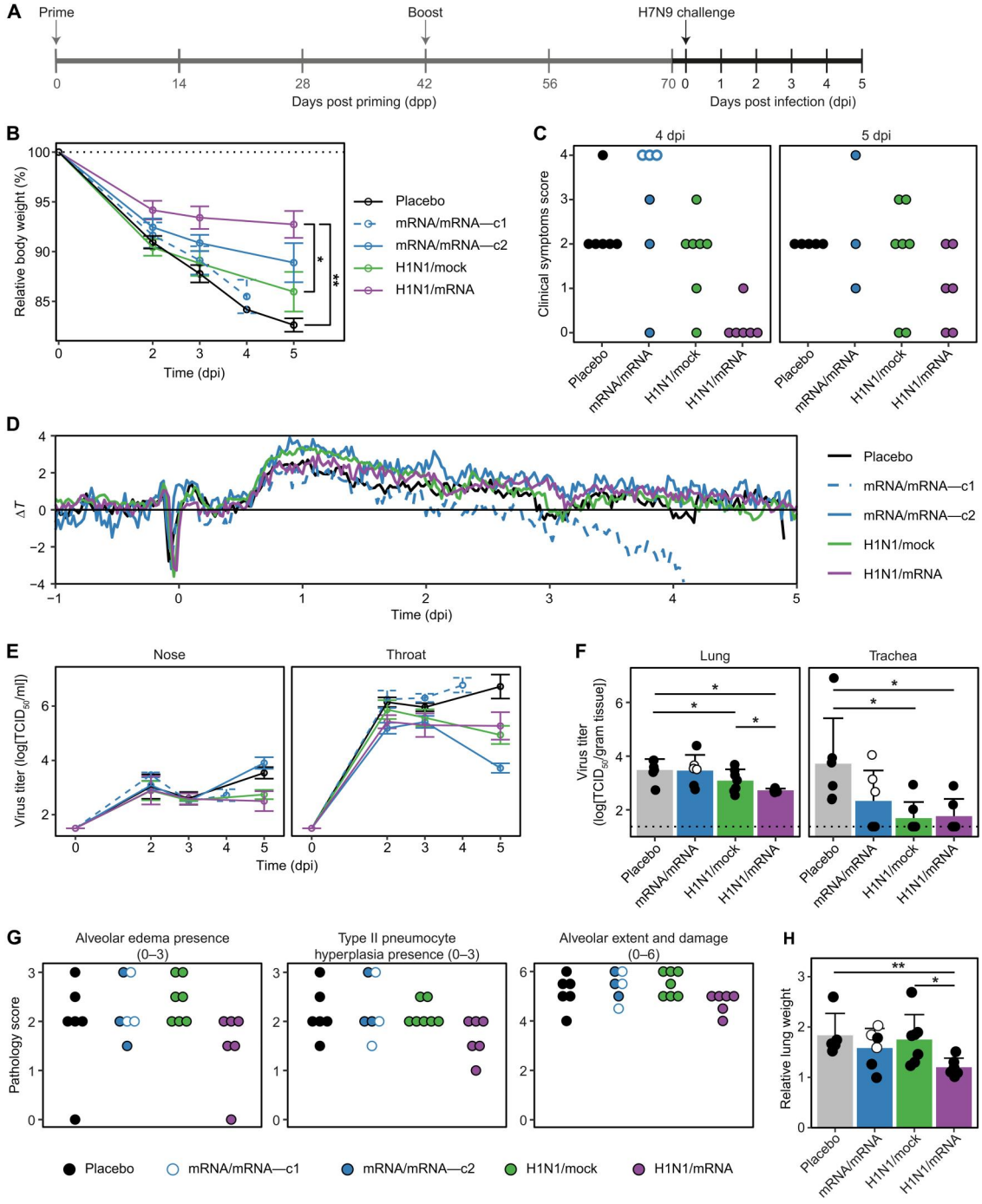

Fig. 4. Boosting of existing immunity increases protection against H7N9 influenza virus challenge. (**A**) Study layout depicting the H7N9 influenza virus challenge after different prime-boost regimens. Ferrets were challenged intratracheally with 10^6 $TCID_{50}$ A/Anhui/1/2013 (H7N9) influenza virus at 71 or 72 dpp, which equals 0 dpi. At 5 dpi, animals were euthanized and tissue pathology and viral loads were assessed. (**B**) Decrease in body weight from 0 to 5 dpi. Body weight is depicted relative to body weight (%) on the day of challenge. (**C**) Clinical scoring for parameter activity and breathing as detailed in Materials and Methods. Ferrets reaching a combined score of 4 have reached the human end points and were euthanized. (**D**) Fever depicted as temperature deviation from baseline. Baseline was determined as average body temperature from −5 to −1 dpi. (**E** and **F**) Viral titers ($TCID_{50}$) in (E) nose and throat swabs and (F) homogenized lung and trachea tissue as determined by end point titration on Madin-Darby canine kidney (MDCK) cells. The dotted line in (F) indicates the limit of detection. (**G**) Pathology scoring for selected parameters as detailed in Materials and Methods. (**H**) Lung weight at 5 dpi relative to body weight on 0 dpi as a derivative of lung inflammation. For all panels, $n = 6$ to 7. (B, E, F, and H) Data are visualized as means ± SD. (D) Data are shown as group means. (C and F to H) Dots represent individual observations of ferrets. One placebo ferret and three mRNA/mRNA-treated ferrets needed to be euthanized 4 dpi because the humane end points were reached. The mRNA/mRNA ferrets euthanized 4 dpi are visualized as separate groups or depicted by open symbols (instead of filled). For visualization purposes, only comparisons between groups placebo, H1N1/mock, and H1N1/mRNA are shown. No statistics were performed for (C) and (G), as these are nominal data. An overview of all statistical comparisons is shown in data file S1. *$P < 0.05$ and **$P < 0.01$.

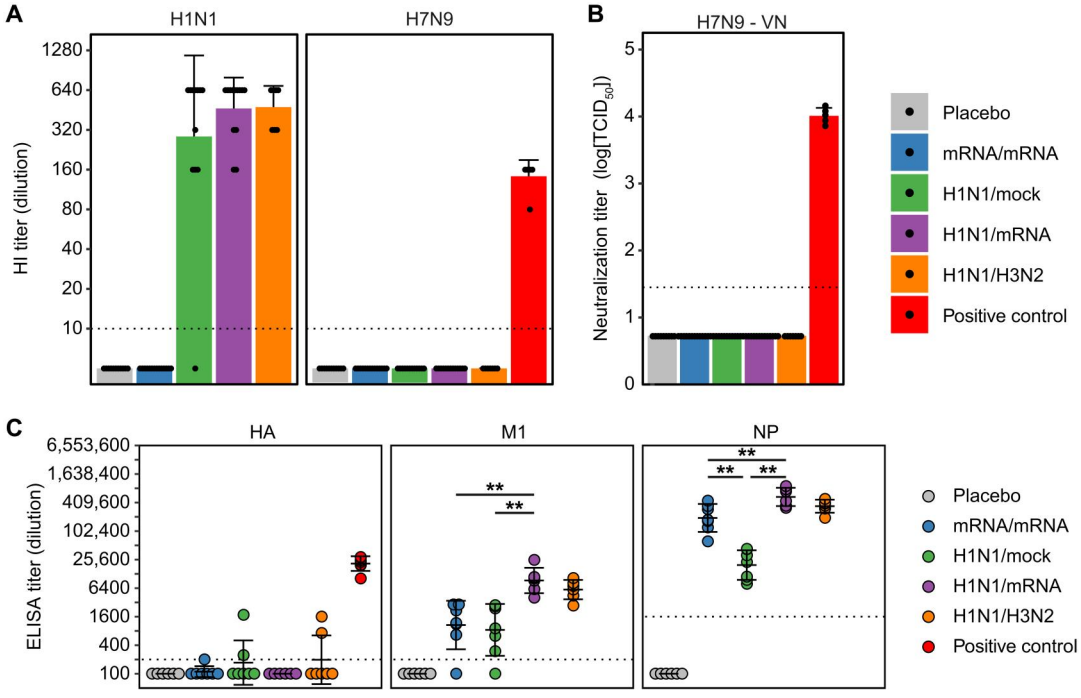

Fig. 5. Antibody responses against H1N1 and H7N9 influenza viruses in sera obtained 70 dpp. (**A**) Antibodies against H1N1 (A/California/07/2009) or H7N9 (H7N9/PR8 reassortant) influenza viruses, measured by HI assay. (**B**) Virus neutralization titer against H7N9 influenza virus. (**C**) Antibodies binding to recombinant HA, M1, or NP of A/Anhui/1/2013 (H7N9) influenza virus measured by ELISA. The antibody titer is calculated as the extrapolated dilution of serum at which the optical density at 450 nm (OD_{450}) drops below background (mean of placebo animals +3× SD). Positive control samples are sera from ferrets previously vaccinated twice with an H7N9 live attenuated virus (*84*). The dotted line represents the lower limit of detection (A and B) or the background cutoff (C). Each dot represents one animal. (A and B) $n = 7$ to 14 (experimental groups) or $n = 5$ (positive control). (C) $n = 6$ to 7. For visualization purposes, only comparisons between groups mRNA/mRNA, H1N1/mock, and H1N1/mRNA are shown in (C). An overview of all statistical comparisons is shown in data file S1. $^{**}P < 0.01$.

the protective capacity of a nucleoside-modified mRNA-LNP vaccine encoding three conserved influenza proteins (mRNA-Flu). To our knowledge, this is the first study that provides a detailed evaluation of an mRNA-based influenza T cell vaccine in a relevant animal model of influenza virus infection.

To mimic the human situation, we tested a combined nucleoside-modified mRNA-LNP vaccine (mRNA-Flu) encoding the internal influenza proteins NP, M1, and PB1 as a prime-boost strategy in naïve ferrets or as a booster in influenza-experienced ferrets. Prime-boost vaccination with mRNA-Flu resulted in robust, broadly reactive cellular responses in the blood, spleen, lungs, NT, and BM, although responses were primarily targeted against NP. mRNA-Flu was even more effective as a booster vaccination in influenza-experienced ferrets, as it enhanced T cell responses in all compartments investigated, including the BAL, and also boosted responses against M1 and PB1. Notably, booster vaccination of H1N1 virus–primed ferrets with mRNA-Flu often induced higher responses (after restimulation) compared to booster by H3N2 influenza virus infection. In H1N1 influenza virus–primed ferrets, mRNA-Flu is a homologous booster, whereas H3N2 infection is a heterologous booster. Despite the high homology of internal proteins of the H3N2 and H1N1 influenza viruses, there may be epitope mismatches that account for the lower response. On the other hand, the response to the internal proteins of an H2N2 virus only resulted in a marginally reduced response to mRNA-Flu–boosted ferrets, indicating that homology may not be the only reason for the occasionally significant differences in T cell responses. These differences may be partly attributed to the performance of the mRNA-Flu vaccine, but further research is required to fully elucidate this observation.

To test the protective effect of the induced immune response, we challenged ferrets with avian H7N9 influenza virus, as this strain has repeatedly transmitted from birds to humans and is considered as potentially pandemic (*50*). After challenge, influenza-experienced ferrets that were boosted with mRNA-Flu lost less weight and showed fewer clinical symptoms, and their lungs contained less severe edema compared to ferrets that did not receive an mRNA-Flu booster vaccination. We did not observe a similar protection for ferrets prime-boosted with mRNA-Flu only, which might be due to less robust and broad T cell responses in the respiratory tract. Still, these results show that our nucleoside-modified mRNA-LNP T cell vaccine is a promising candidate to boost broadly reactive cellular responses and can be used to enhance protection against heterosubtypic influenza viruses.

We have previously shown that both ferrets and healthy human blood donors have clearly detectable NP-, M1-, and PB1-reactive T cells (*24*). In our current experimental model, both a single mRNA-Flu vaccination and H1N1 influenza virus infection elicited NP-specific responses. Responses against M1 and PB1 were weaker, especially in mRNA-Flu–primed animals. However, booster vaccination increased M1- and PB1-specific responses in all H1N1-primed ferrets, and approximately half of the mRNA/mRNA ferrets developed detectable M1- and PB1-specific responses. Although it is unclear why M1- and PB1-specific immunity was weak initially,

these responses substantially increased shortly after H7N9 influenza virus challenge, suggesting that M1- and PB1-specific T cells played a role in reducing H7N9 influenza disease. This indicates that it could be beneficial if future mRNA-based influenza vaccines targeted multiple relatively well-conserved internal proteins. This would also safeguard against influenza virus mutations, as the virus is less likely to escape from a broad immune response.

The T cells induced by mRNA-Flu vaccination responded to a wide range of influenza viruses, including seasonal H3N2, pandemic H2N2, and avian H5N1 and H7N9 strains. A previous research has already shown that T cells, especially lung resident memory T cells (T_{RM}), are crucial for protection against heterosubtypic infections (*47*, *51*). We show that mRNA-LNP vaccination, in contrast to inactivated influenza vaccines (*52*), is able to induce T cells residing in the respiratory tract, even when given intramuscularly. Whether these T cells have a T_{RM} phenotype still remains to be elucidated because of the lack of ferret-specific reagents. The T cell responses that we found in NT and lung after mRNA-Flu prime boost confirms a previous report of Laczko *et al.* (*53*) who found that intramuscular administration of mRNA-LNP vaccines induced potent cellular responses in the lungs of mice. The responses that we found were not an artifact of circulating lymphocytes, as lungs were perfused and cellular responses in the lungs were higher than those in the blood, showing that influenza virus–specific T cells accumulated in the lung tissue. Still, responses in the BAL were absent in mRNA-Flu prime-boosted ferrets, indicating that local presentation of antigen and/or inflammation is required for extended tissue-residing cellular immunity. Intranasal administration of mRNA vaccines could potentially enhance protection by also inducing T cells in the BAL and increasing T cell numbers in the NT, but additional research needs to be performed to overcome the epithelial barrier and to prevent excessive immune activation (*54*). mRNA-Flu vaccination boosted cellular responses in the BAL, NT, and lungs of H1N1-primed ferrets that reacted not only to NP but also to M1 and PB1. This is a particularly relevant finding, as a large part of the human population has already been naturally exposed to influenza virus. For this group, a single mRNA-LNP immunization administered intramuscularly may be sufficient to boost respiratory T cell responses. These findings stress the importance of animal models that reflect the human infection history, as preexisting immunity can clearly influence vaccine responses.

mRNA-Flu also induced potent responses in the BM. This may be partly caused by the close proximity of mRNA-Flu administration (hind legs) and T cell isolation from the BM (femur). T cells can be primed in the BM after local antigen presentation (*55*, *56*). This can be beneficial for the longevity of the cellular response, as the BM serves as a reservoir for memory T cells (*57*, *58*). The observation that nucleoside-modified mRNA-LNP vaccination is a potent inducer of BM-residing T cell immunity warrants further investigations into the longevity and importance of this response.

In our study, vaccine-induced T cell responses consisted of both $CD4^+$ and $CD8^+$ T cells. Similarly, Freyn *et al.* (*40*) found that a single dose of H1N1 NA- or NP-encoding mRNA-LNP induced robust $CD4^+$ and $CD8^+$ T cell responses in mice. In humans, SARS-CoV-2 mRNA-LNP vaccines also induced both $CD4^+$ and $CD8^+$ T cells, although the extent to which the vaccines induced $CD4^+$ and $CD8^+$ T cells differs between studies (*34*, *59*, *60*). We found that the T cell response after mRNA-Flu booster vaccination was skewed toward a $CD8^+$ phenotype. This skewing might be beneficial, as clearing virus-infected cells is primarily mediated by $CD8^+$ T cells (*19*). It should be mentioned, however, that we could only measure IFN-γ responses, and we might have missed activated $CD4^+$ T cells that responded by producing other typical $CD4^+$ cytokines such as tumor necrosis factor and interleukin-2.

Besides T cells, the mRNA-Flu vaccine also induced humoral responses against NP, M1, and possibly PB1; antibodies against PB1 could not be measured because of the lack of reagents. We did not find any functional role for NP and M1 antibodies by HI and VN assays, although these assays primarily detect (neutralizing) anti-HA antibodies. Still, in mice, vaccination with recombinant NP protein induced potent anti-NP antibodies that protected against severe disease after an influenza virus challenge but only if these mice also had functional T cells (*61*, *62*). This protection may be mediated by antibody-dependent cell cytotoxicity (ADCC) activity, although it is still uncertain whether NP- and M1-specific antibodies can facilitate ADCC (*63*, *64*). Whether ADCC or other effector mechanisms played a role in our study remains therefore unknown. Future serum transfer experiments in ferrets could help in clarifying the exact role of NP-, M1-, and PB1-specific antibodies in the protection against influenza virus disease.

To evaluate the robustness of T cell–mediated protective immunity, we used a ferret challenge model in which a lethal dose of H7N9 influenza virus was deposited directly into the lungs of animals by intratracheal inoculation. In this way, a large amount of pneumocytes become directly infected, and T cells are only granted a short time frame to become activated and prevent further disease. This robust challenge model is not representative of a normal human exposure. People typically encounter a lower viral load (*65*) and primarily in the upper respiratory tract, which affords T cells a longer time to establish protective immunity. We thus expect a greater protective effect of the T cell response upon natural infection doses. The challenge model that we used, while not using a natural inoculation route and dose, very well represents the severe pneumonia observed in humans hospitalized with H7N9 influenza virus infection, which cannot be achieved with lower infection doses and other inoculation routes. Because the ferrets in this study were infected and boosted in a relatively short time span (6 weeks), future studies should investigate whether the boost in the T cell immunity and protection against disease are affected when the interval between infection and vaccination is increased (e.g., 6 months).

We could not clearly establish whether a prime-boost strategy with mRNA-Flu was protective likely because of a cage effect. Ferrets prime-boosted with mRNA-Flu housed in one isolator showed protection against H7N9 influenza disease similarly to mRNA-Flu–boosted influenza-experienced ferrets. Ferrets in the second isolator however showed more severe symptoms after infection than the placebo animals and needed to be euthanized 1 day before the scheduled termination of the experiment. We did not find differences between the two cages that explain this discrepancy. Both humoral and cellular immune responses were similar, ferrets tested negative for Aleutian disease and showed similar previous exposure to canine distemper virus and ferret corona viruses. For practical reasons, the H7N9 influenza virus challenge was performed on two consecutive days with each treatment group split over both days (see Materials and Methods for details). It is unlikely that differences are due to separate preparation of the inoculum, as all other groups, which were also divided over 2 days, did not

respond differently to the challenge. Additional experiments would be required to clarify whether the influenza-specific T cell response induced by prime-boost vaccination with mRNA-Flu is protective in ferrets.

In contrast to traditional inactivated influenza virus vaccines that usually induce weak cellular immune responses, nucleoside-modified mRNA-LNP vaccines can effectively induce both humoral and cellular immunity (*34*–*38*). With the induction of a broadly reactive T cell response, universal influenza mRNA vaccines should be less sensitive to antigenic drift and shift that hamper traditional HA-based vaccines. Furthermore, mRNA-LNP SARS-CoV-2 vaccines perform well in elderly people (*66*, *67*), while inactivated influenza virus vaccines often have subpar performance with increasing age (*68*). Results from a recent clinical trial with a quadrivalent HA-based mRNA vaccine did not show superior immunogenicity of this mRNA vaccine to a registered high-dose influenza vaccine (*69*). The true potential of mRNA vaccines, however, partly lies in their ability to induce both robust humoral and cellular immunity. The addition of conserved T cell epitopes to mRNA-based influenza vaccines might thus be a viable option to protect influenza-experienced individuals that are at high risk for influenza-related mortality and morbidity, especially in cases where the seasonal vaccine strains do not match with the circulating viruses. The inclusion of conserved internal influenza virus proteins could additionally provide protection against potential pandemic influenza viruses, as shown in the current study. As demonstrated in the COVID-19 pandemic, additional advantages of the mRNA vaccine platform are the flexibility of vaccine design and the highly scalable, rapid production (*33*).

Recently, two clinical studies investigating universal influenza T cell vaccines did not improve protection from viral infection. One of these vaccines was protein-based (*70*), which, by definition, does not induce endogenous protein synthesis required for efficient induction of cytotoxic cellular immunity. This caveat can be overcome by the nucleoside-modified mRNA-LNP platform that was demonstrated to induce robust $CD8^+$ T cell responses in our preclinical experiments and in clinical mRNA vaccine studies for SARS-CoV-2 (*40*, *53*, *71*). In another study, a modified vaccinia Ankara vector expressing NP and M1 (MVA-NP-M1) was used in addition to standard seasonal vaccination (*30*). The use of a well-matching seasonal vaccine resulted in a relatively good effectiveness; therefore, it is possible that the seasonal vaccine–induced antibodies masked the effect of the cellular response induced by MVA-NP-M1. This study indicates that we should carefully consider the conditions under which we evaluate universal vaccines, as universal cellular immunity is more likely to show a robust effect when the antibody response is suboptimal, e.g., when there is a mismatch or introduction of a new antigenically distinct influenza virus (*72*).

To our best knowledge, this is the first study that provides a detailed evaluation of an mRNA-based combined influenza T cell vaccine in a highly relevant ferret model. We postulate that the nucleoside-modified mRNA-LNP–based influenza vaccine can boost the number of broadly reactive T cells to a level that prevents severe influenza disease and death, reducing the impact of future influenza epidemics and pandemics on the society.

MATERIALS AND METHODS

Ethics statement

The experiment was approved by the Animal Welfare Body of Poonawalla Science Park–Animal Research Center (Bilthoven, The Netherlands) under permit number AVD3260020184765 of the Dutch Central Committee for Animal Experiments. All procedures were conducted according to the European Union legislation. Ferrets were examined for general health on a daily basis. If animals showed severe disease according to the defined end points before scheduled termination, then they would be euthanized by cardiac bleeding under anesthesia with ketamine (5 mg/kg; Alfasan, Woerden, The Netherlands) and medetomidine (0.1 mg/kg; Orion Pharma, Espoo, Finland). End points were scored on the basis of clinical parameters for activity (0, active; 1, active when stimulated; 2, inactive; and 3, lethargic) and impaired breathing (0, normal; 1, fast breathing; and 2, heavy/stomach breathing). Animals were euthanized when they reached score 3 on activity level (lethargic), when the combined score of activity and breathing impairment reached 4, or if their body weight decreased by more than 20%.

Cell and virus culture

Madin-Darby canine kidney (MDCK) cells were grown in minimum essential medium (MEM) (Gibco, Thermo Fisher Scientific, Waltham, MA) supplemented with 10% fetal bovine serum (FBS; HyClone, GE Healthcare, Chicago, IL), gentamicin (40 μg/ml), and 0.01 M Tricine (both from Sigma-Aldrich, Saint Louis, MO). Vero E6 cells were cultured in Dulbecco′s modified Eagle′s medium (DMEM; Gibco) supplemented with 10% FBS and 1× penicillin-streptomycin-glutamine (Gibco). A/California/07/2009 (H1N1), A/Switzerland/97-15293/2013 (H3N2), A/Vietnam/1203/2004 WT (H5N1), A/Anhui/1/2013 (H7N9), and H7N9/PR8 reassortant (NIBRG-268, NIBSC code 13/250) influenza viruses were obtained from the National Institute for Biological Standards and Control (NIBSC, Hertfordshire, England). Influenza virus was grown on MDCK cells in MEM supplemented with gentamicin (40 μg/ml), 0.01 M Tricine, and tosyl phenylalanyl chloromethyl ketone–treated trypsin (2 μg/ml; Sigma-Aldrich). At >90% cytopathic effect (CPE), the suspension was collected and spun down (4000*g* for 10 min) to remove cell debris. H1N1 and H3N2 virus were sucrose-purified on a discontinuous 10 to 50% sucrose gradient. Because of the Biosafety Level 3 (BSL-3) classification of H7N9 and H5N1, the virus was not purified. All virus aliquots were snap-frozen and stored at −80°C.

mRNA production

NP, M1, and PB1 mRNAs are based on the A/Michigan/45/2015 H1N1pdm virus, which is nearly identical to A/California/07/2009 (NP = 99.2%, M1 = 98.4%, and PB1 = 99.6% conserved). Production of mRNAs was performed as described earlier (*40*, *73*). Briefly, codon-optimized NP, M1, and PB1 genes were synthesized (GenScript, Piscataway, NJ) and cloned into an mRNA production plasmid. T7-driven in vitro transcription reactions (MEGAscript, Ambion, Thermo Fisher Scientific) using linearized plasmid templates were performed to generate mRNAs with 101-nucleotide-long polyadenylate tails. Capping of mRNAs was performed in concert with transcription through the addition of a trinucleotide cap1 analog, CleanCap (TriLink, San Diego, CA). m1Ψ-5′-

triphosphate (TriLink) was incorporated into the mRNA instead of uridine 5′-triphosphate. Cellulose-based purification of mRNAs was performed as described (*74*). mRNAs were then tested on an agarose gel before storing at −20°C.

LNP formulation of mRNA

Purified mRNAs were formulated into LNP using a self-assembly process wherein an ethanolic lipid mixture of an ionizable cationic lipid, phosphatidylcholine, cholesterol, and polyethylene glycol lipid was rapidly combined with an aqueous solution containing mRNA at an acidic pH as previously described (*46*). The ionizable cationic lipid [pK_a (where K_a is the acid dissociation constant) in the range of 6.0 to 6.5; proprietary to Acuitas Therapeutics, Vancouver, Canada] and LNP composition are described in the patent application WO 2017/004143. The average hydrodynamic diameter was ~80 nm with a polydispersity index of 0.02 to 0.06 as measured by dynamic light scattering using a Zetasizer Nano ZS (Malvern Instruments Ltd., Malvern, UK) and an encapsulation efficiency of ~95% as determined using a RiboGreen assay.

Cell transfections and Western blot analysis of mRNA-LNPs

Cell transfection of HEK293T cells was performed with TransIT-mRNA (Mirus Bio, Madison, WI) as described before (*44*). Briefly, mRNA (0.3 μg) was combined with TransIT-mRNA Reagent (0.34 μl) and Boost Reagent (0.22 μl) in 17 μl of serum-free medium, and the complex was added to 6×10^4 cells in 183 μl of complete medium.

Cell lysates of firefly luciferase, M1, or PB1 mRNA-transfected and nontransfected HEK293T cells were used for Western blotting. Cells were collected 24 hours after transfection and lysed for 1 hour on ice in radioimmunoprecipitation assay buffer (Sigma-Aldrich). Samples were combined with 355 mM 2-mercaptoethanol (Bio-Rad, Hercules, CA) containing 4× Laemmli buffer (Bio-Rad) and were boiled for 5 min and spun at 18,000*g* for 5 min at room temperature. The samples were separated on a 4 to 15% precast polyacrylamide Criterion TGX gel (Bio-Rad) for 45 min at 200 V. Transfer to polyvinylidene difluoride membrane (Thermo Fisher Scientific) was performed using a semidry apparatus (Bio-Rad) at 10 V for 1 hour. The membrane was blocked in 5% milk powder–TBST [25 mM tris, 150 mM NaCl (pH 7.5), and 0.1% Tween 20] for 1.5 hours, and then, the membrane was incubated with the anti-M1 (mouse monoclonal, 1:5000; Thermo Fisher Scientific, #MA1-80736), anti-PB1 (rabbit polyclonal, 1:5000; Thermo Fisher Scientific, #PA5-34914), and anti–glyceraldehyde-3-phosphate dehydrogenase (rabbit monoclonal, 1:10,000; Cell Signaling Technology, Danvers, MA, #2118) primary antibodies overnight at 4°C. The membrane was washed with 1× TBST for 30 min and incubated with the horseradish peroxidase (HRP)–conjugated anti-rabbit (goat polyclonal, 1:10,000; Thermo Fisher Scientific, #31458) or anti-mouse (donkey polyclonal, 1:10,000; Jackson ImmunoResearch, #715-035-150) secondary antibodies for 1 hour at room temperature. After washing three times for 20 min with 1× TBST at room temperature, the signal was developed with the HRP substrate solution (GE Healthcare, Amersham ECL Western Blotting Detection Reagents) and imaged using an Amersham Imager 680 (GE Healthcare) machine.

Animal handling

Sixty-three female ferrets (*Mustela putorius furo*) aged 12 to 13 months (Euroferret, Copenhagen, Denmark) were delivered 3 weeks before commencement of the study and were semirandomly distributed by weight. Ferret throat swabs were screened for SARS-CoV-2 by reverse transcription–quantitative polymerase chain reaction (RT-qPCR) as described before (*75*), and ferret sera was screened for influenza exposure by NP ELISA (Innovate Diagnostics, Grabels, France) and HI. In addition, ferret sera (ELISA) and swabs (RT-qPCR) were screened for other corona viruses, canine distemper virus, and Aleutian disease by the European Veterinary Laboratory (Woerden, the Netherlands). All ferrets tested negative for influenza and SARS-CoV-2. Four animals displayed low antibody titers against Aleutian disease. All animals had titers for canine distemper virus antibodies but tested negative for active infection by RT-qPCR. Ferrets were housed per three or four animals in open cages and received pelleted food (Altromin 5539) and water ad libitum. Animals were visually inspected daily and weighed at least once per 7 days. Light was adjusted to 9.5 hours per day to prevent the ferrets from going into estrous. For influenza infections, animals were moved to BSL-3 level isolators. Because of a limited number of isolators, groups that did not receive an infection were kept housed in regular open cages. Fourteen days after infection, the animals were confirmed to be negative for infectious influenza and moved back to regular housing.

Ferrets that received a (mock) infection were swabbed and weighed at 0, 2, 4, 7, 9, and 14 days after the first and second infection. Vaccinated animals were only swabbed at days 0 and 14 and weighed on days 0, 7, and 14. Blood was collected from the vena cava at 0, 14, 28, 42, 56, and 71 dpp. These handlings were performed under anesthesia with ketamine (5 mg/kg). Blood was collected by heart puncture on 70 and 76 dpp. Infections, vaccinations, temperature transponder implantation, and euthanasia were performed after anesthetization with ketamine and medetomidine (0.1 mg/kg). Animals that received a temperature transponder (Star-Oddi, Garðabær, Iceland) abdominally received 0.2 ml of Buprenodale (AST Farma, Oudewater, The Netherlands) as a postoperative analgesic. Anesthesia with medetomidine was antagonized with atipamezole (0.25 mg/kg; Orion Pharma) but was delayed by 30 min in case of infection/vaccination to prevent sneezing and coughing.

Study outline

The study consisted of five experimental groups: (i) placebo, (ii) mRNA/mRNA, (iii) H1N1/mock, (iv) H1N1/mRNA, and (v) H1N1/H3N2. Each experimental group consisted of 14 (groups 1 to 4) or 7 (group 5) ferrets. For practical reasons, the experiment was split into three subexperiments (A, B, and CD). All subexperiments followed the same regime up to day 70 of the experiment but were started 8 days after each other. Subexperiments A and B both contained groups 1 to 5 with three to four animals per group and were terminated 70 dpp to study the immune response. Subexperiment CD contained groups 1 to 4 with seven animals per group, split over two cages. Subexperiment CD was again dived into two smaller subexperiments (C and D) on 71 dpp, which were challenged with H7N9 on 71 and 72 dpp, respectively. Data from the different subexperiments were visualized and analyzed together.

On day 0, groups 3 to 5 were inoculated intranasally with 10^6 $TCID_{50}$ H1N1 in 0.1 ml of inoculum. Group 1 received PBS in

the same manner. Group 2 was administered 250 μl of mRNA vaccine, containing 50 μg of NP, M1, and PB1 mRNA-LNP, in their left or right hind leg. On 42 dpp, animals received a booster treatment. Group 5 was inoculated intranasally with 10^6 $TCID_{50}$ H3N2 in 0.1 ml of inoculum. Group 1 was treated similarly but received PBS instead of H3N2 virus. Groups 2 to 4 were injected with 250 μl of influenza-mRNA vaccine (groups 2 and 4) or Luciferase-mRNA (group 3; 50 μg) in their left or right hind leg. At 70 dpp, seven ferrets of each group were euthanized to study the immune response in the respiratory tract. The other seven animals (excluding group 5) were challenged intratracheally with 10^6 $TCID_{50}$ H7N9 in 3 ml of inoculum at 71 or 72 dpp. Five days later, ferrets were euthanized to study viral titers and pathology.

Animals were euthanized by heart puncture, and blood and serum were collected. For ferrets in subexperiments A and B, the lungs were perfused as described before (*24*), and BAL was collected by flushing the lungs twice with 30 ml of room temperature RMPI 1640 (Gibco). The BAL fluid was then kept on ice until processing. Lungs, spleen, femur (right leg), and NTs were collected in cold RMPI 1640 supplemented with 10% FBS and 1× penicillin-streptomycin-glutamine and stored at +4°C until processing. For ferrets in subexperiments C and D, lungs were weighed before the left cranial and caudal lobes were inflated with and stored in 10% formaldehyde for later pathological analysis. Small slices of the right cranial, middle, and caudal lobes were put in Lysing Matrix A tubes (MP Biomedicals, Irvine, CA) and stored at −80°C until later virological analysis. The lower part of the trachea was stored in 10% formaldehyde for pathology, and 1 cm of the middle part of the trachea was stored in Lysing Matrix A tubes.

Tissue processing

Blood was collected in 3.5-ml VACUETTE tubes with clot activator (Greiner, Merck, Kenilworth, NJ) and spun down at 4000*g* for 10 min to isolate the serum. Heparin blood was collected in 9-ml sodium heparin–coated VACUETTE tubes (Greiner) and diluted 1:1 with PBS (Gibco) for density centrifugation on a 1:1 mixture of LymphoPrep (1.077 g/ml; STEMCELL Technologies, Vancouver, Canada) and Lympholyte-M (1.0875 g/ml; Cedarlane, Burlington, Canada). Cells were spun for 30 min at 800*g*, after which the interphase was collected and washed thrice with a washing medium (RPMI 1640 + 1% FBS + 1× penicillin-streptomycin-glutamine). Next, cells were resuspended in stimulation medium (RPMI 1640 + 10% FBS + 1× penicillin-streptomycin-glutamine) and counted using a hemocytometer.

Spleen, lung, and NT tissue were processed as detailed before (*24*). Briefly, spleens were homogenized in a sieve using the plunger of a 10-ml syringe. The resulting suspension was collected while excluding the larger debris and pelleted by centrifugation for 10 min at 500*g*. The pellet was resuspended in 50 ml of EDTA-supplemented (2 mM) washing medium and transferred over a 100-μm SmartStrainer (Miltenyi Biotec, Bergisch Gladbach, Germany). The cell suspension was then diluted to 90 ml, which was divided into 3 × 30 ml and layered on top of 15 ml of Lympholyte-M for density centrifugation similar to that of the blood. All washing steps were performed with an EDTA-supplemented medium to prevent agglutination of cells.

Lungs were cut into 5-mm^3 cubes and digested in 12 ml of collagenase I (2.4 mg/ml; Merck) and deoxyribonuclease I (DNase I; 1 mg/ml; Novus Biologicals, Centennial, CO) for 60 min at 37°C while rotating. Samples were homogenized in a sieve using a plunger, spun down for 10 min at 500*g*, and resuspended in washing medium. This suspension was transferred over a 70-μm cell strainer (Greiner) and used for density centrifugation similar to that of the spleen.

NTs were mashed on a sieve using a plunger and pelleted by spinning for 5 min at 500*g*. The pellet was resuspended in 3 ml of collagenase/DNase solution (similar to lung) and incubated for 30 min at 37°C while rotating. Next, the suspension was directly mashed over a 70-μm cell strainer (Greiner) with a plunger and washed twice with 10 ml of washing medium. The resulting pellet was resuspended in 6 ml of 40% Percoll (GE Healthcare) and layered on top of 70% Percoll to isolate the leukocytes. Samples were spun for 20 min at 500*g*, after which the interphase was collected and washed twice with washing medium. After the final wash, cells were resuspended in stimulation medium and used for ELISpot and fluorescence-activated cell sorting (FACS).

After collection, 3 ml of BAL was used for ELISpot without further processing. The remaining volume was spun down at 500*g* for 5 min and resuspended in 12 ml of FACS buffer [PBS (Gibco) + 0.5% bovine serum albumin (Merck) + 2 mM EDTA]. The suspension was transferred over a 70-μm SmartStrainer (Miltenyi Biotec), spun down at 500*g* for 5 min, and resuspended in FACS buffer. This suspension was used for flow cytometry.

Femurs were cleaned from residual tissues and briefly decontaminated with 70% ethanol. The femur was then cut on both sides so that the shaft could be flushed with 15 ml of ice-cold RPMI washing medium. The suspension was transferred over a 70-μm cell strainer and pelleted by centrifugation for 7 min at 500*g* at 4°C. Erythrocytes were lysed with ACK Lysis Buffer after which the suspension was spun down, resuspended in washing medium, and again transferred over a 70-μm cell strainer. The resulting suspension was spun down, resuspended in stimulation medium, and used for ELISpot and flow cytometry.

Peptide pools

NP (NR-18976), M1 (NR-21541), and PB1 (NR-18981) H1N1 peptide arrays were obtained through BEI Resources, National Institute of Allergy and Infectious Diseases, NIH. Peptide libraries for H1N1 NP, M1, and PB1 were based on A/California/04/2009, which is 100% identical (for NP, M1, and PB1) to the A/California/07/2009 strain that we used for the infection. Peptides were supplied as individual aliquots and were pooled in-house after dissolving in H_2O, 50% acetonitrile, or dimethyl sulfoxide (DMSO) depending on the solvability. The merged peptide suspension was then aliquoted and speed-vacced for 48 hours to reduce the volume. Vials were stored at −80°C.

H2N2 peptide pools were based on A/Leningrad/134/17/1957 and were custom-ordered from JPT Peptide Technologies GmbH (Berlin, Germany). Each pool contained 15–amino acid–long peptides with an overlap of 11 amino acids spanning the entire protein of NP, M1, or PB1. Peptides were synthesized as reported before (*24*). HIV-1 Con B gag motif peptide pool (JPT) served as a negative control for our assays and was handled the same way as the H2N2 peptide pools.

Before use, H1N1 and H2N2 peptide pools were dissolved in DMSO, aliquoted, and stored at −20°C. On the day of use, peptide pool aliquots were thawed and diluted with stimulation medium. The peptide pool suspension was added to cells such

that a final peptide concentration of 1 μg/ml per peptide with a DMSO concentration of less than 0.2% was achieved.

ELISpot

Precoated Ferret IFN-γ ELISpot (ALP) plates (Mabtech, Nacka Strand, Sweden) were used according to the manufacturer's protocol. Lymphocytes were stimulated with live virus [multiplicity of infection (MOI) of 100 for H3N2, MOI of 1 for H5N1, and MOI of 0.1 for H1N1 and H7N9] or peptide pools (1 μg/ml) in ELISpot plates at 37°C. Per well, 250,000 cells (PBMCs), 400,000 cells (BM), 62.5,000 cells (lung lymphocytes), or undiluted cell suspension (BAL and NTs) was added. On day 56 to 2 weeks after booster vaccination, 125,000 PBMCs were used for viral stimulations because of high cellular responses. After 20 hours, the plates were developed according to the manufacturer's protocol, with the modification that the first antibody staining was performed overnight at 4°C. Plates were left to dry for 2 to 3 days, after which they were packaged under BSL-3 conditions and heated to 65°C for 3 hours to inactivate any remaining infectious influenza particles. Analysis of ELISpot plates was performed using the ImmunoSpot S6 Core (CTL, Cleveland, OH).

Flow cytometry: Cell counts

BAL and NT samples were stained in 96-well plates using the Forkhead Box P3 (FoxP3)/transcription factor staining buffer set (eBioscience, Thermo Fisher Scientific). Cells were stained with α-CD4–allophycocyanin (02, Sino Biological, Beijing, China), α-CD8a–eFluor450 (OKT8, eBioscience), α-CD14–phycoerythrin (Tük4, Thermo Fisher Scientific), and Fixable Viability Stain 780 (BD, Franklin Lakes, NJ) in 100 μl for 30 min at 4°C. Samples were then washed twice with 150 μl of FACS buffer, followed by fixation with 100 μl of fixative from the FoxP3 staining kit for 20 min at room temperature. Next, samples were washed twice with 150 μl of 1× permeabilization buffer (FoxP3 staining kit). After the second wash, samples were stained with 100 μl of permeabilization buffer containing α-CD3e–fluorescein isothiocyanate (CD3-12, Bio-Rad) for 30 min at 4°C. Samples were then washed twice with 150 μl of 1× permeabilization buffer and once with 150 μl of FACS buffer. After the last wash, samples were resuspended in 180 μl of FACS buffer, after which 50 μl of precision count beads (BioLegend, San Diego, CA) were added to BAL and NT samples. Samples were measured in plates using the high-throughput system of a Symphony A3 system (BD). Data were analyzed using FlowJo Software v.10.6 (BD).

Flow cytometry: Intracellular cytokine staining

Lymphocytes derived from blood, lungs, or BM were stimulated in U-bottom plates with 1 million to 3 million cells per well. Stimulations consisted of medium; H1N1 live virus (MOI of 1); H3N2 live virus (MOI of 10); an H1N1 peptide cocktail containing peptide pools of NP, M1, and PB1 (1 μg/peptide/ml); and an HIV peptide pool (1 μg per peptide per ml) serving as a negative control. Cells were stimulated for 20 (virus, medium) or 6 hours (peptide pools) at 37°C. During the last 5 hours of stimulation, 1× brefeldin A (BioLegend) was added to each well. Plates were then stored at 4°C until they were stained the following morning. Staining and acquisition followed the same procedure as detailed above, with the exception that α-CD14–PE was absent in the extracellular staining and instead, α-IFN-γ–R-phycoerythrin (CC302, MyBioSource, San Diego, CA) was added to the intracellular staining.

$TCID_{50}$ determination

Nose and throat swabs were collected in 2 ml of transport medium containing 15% sucrose (Merck), amphotericin B (2.5 μg/ml), penicillin (100 U/ml), streptomycin (100 μg/ml), and gentamicin (250 μg/ml) (all from Sigma-Aldrich) and stored at −80°C. For analysis, swabs were thawed, vortexed, serially diluted, and tested in sextuplicate on MDCK cells. Trachea and lung samples stored in Matrix A tubes were thawed, and 750 μl of DMEM infection medium (DMEM containing 2% FBS and 1× penicillin-streptomycin-glutamine) was added. Tissues were then dissociated in a FastPrep-24 by shaking twice for 1 min, after which the samples were spun down for 5 min at 4000*g*. To determine viral titers, the supernatant was serially diluted in sextuplicate on MDCK cells. CPE was scored after 6 days of culturing, and $TCID_{50}$ values were calculated using the Reed and Muench method. Viral titers in virus stocks were similarly tested but in octuplicate.

Enzyme-linked immunosorbent assay

Immulon 2 HB 96-well plates (Thermo Fisher Scientific) were coated overnight at room temperature with 100 μl per well of recombinant HA (0.5 μg/ml), NP (0.5 μg/ml), or M1 (0.25 μg/ml) protein of A/Anhui/1/2013 (Sino Biologicals). The next day, plates were washed thrice with PBS + 0.1% Tween 80 before use. Sera were diluted 1:100 in PBS + 0.1% Tween 80 and then twofold serially diluted. Per well, 100 μl of diluted sera was added, and plates were incubated for 60 min at 37°C. After washing thrice with 0.1% Tween 80, plates were incubated for 60 min at 37°C with HRP-conjugated goat anti-ferret immunoglobulin G (IgG; Alpha Diagnostic) and diluted 1:5000 in PBS containing 0.1% Tween 80 and 0.5% Protifar (Nutricia, Hoofddorp, The Netherlands). Plates were then washed trice with PBS + 0.1% Tween 80 and once with PBS, followed by development with 100 μl of SureBlue TMB (KPL, Gaithersburg, MD) substrate. Development was stopped after 10 min by the addition of 100 μl of 2 M H_2SO_4, and OD_{450} (optical density at 450 nm) values were determined on the EL808 absorbance reader (Bio-Tek Instruments). Individual curves were visualized using local polynomial regression fitting with R software v.4.1.1 (*76*). Antibody titers were determined as the dilution at which antibody responses dropped below background. This background was calculated as the "mean + 3 × SD" of the OD_{450} at a 200× (HA and M1) or 1600× (NP) serum dilution of placebo animals.

HI assay

HI titers in ferret sera were determined in duplicate according to the World Health Organization (WHO) guidelines (*77*). Briefly, sera were heat-inactivated at 56°C for 30 min and treated with a receptor-destroying enzyme (Sigma-Aldrich) in a 1:4 mixture (5× dilution of sera). Sera were then twofold serially diluted in PBS and mixed 1:1 with four hemagglutinating units of H1N1 or H7N9 in 96-well plates (starting dilution, 1:10). The serum-virus mixture was incubated for 20 min at room temperature, followed by the addition of 0.5% turkey red blood cells (bioTRADING) in a 1:1 mixture. Samples were incubated for 45 min at room temperature, after which agglutination was scored.

VN assay

VN titers were determined as described previously (*78*) and according to WHO guidelines (*77*). Sera were inactivated (30 min at 56°C) and twofold serially diluted in virus growth medium using a starting dilution of 1:8. Virus at a concentration of 100 $TCID_{50}$ was added, and the mixture was incubated for 2 hours at 37°C. Next, the virus-serum mixture was transferred to 96-well plates containing confluent MDCK cells and incubated for another 2 hours at 37°C, after which the medium was refreshed. Plates were incubated until a back titration plate reached CPE at a titer of 100 $TCID_{50}$ (4 to 5 days). The 50% VN titers per milliliter of serum was calculated by the Reed and Muench method (*79*).

Pathology

Tissues harvested for histological examination (trachea, bronchus, and left lung) were fixed in 10% neutral-buffered formalin, embedded in paraffin, sectioned at 4 μm, and stained with hematoxylin and eosin for examination by light microscopy. Semiquantitative assessment of influenza virus–associated inflammation in the lung (four slides with longitudinal section or cross section of cranial or caudal lobes per animal) was performed on every slide as reported earlier (*80*) with few modifications: For the extent of alveolitis and alveolar damage, we used the following: 0, 0%; 1, 1 to 25%; 2, 25 to 50%; and 3, >50%. For the severity of alveolitis, bronchiolitis, bronchitis, and tracheitis, we scored the following: 0, no inflammatory cells; 1, few inflammatory cells; 2, moderate numbers of inflammatory cells; and 3, many inflammatory cells. For the presence of alveolar edema and type II pneumocyte hyperplasia, we scored the following: 0, 0%; 1, <25%; 2, 25 to 50%; and 3, >50%. For the presence of alveolar hemorrhage, we scored the following: 0, no and 1, yes. For the extent of peribronchial/perivascular edema, we scored the following: 0, no and 1, yes. Last, for the extent of peribronchial, peribronchiolar, and perivascular infiltrates, we scored the following: 0, none; 1, 1 to 2 cells thick; 2, 3 to 10 cells thick; and 3, more than 10 cells thick. Slides were examined without knowledge of the treatment allocation of the animals.

Body temperature, body weight, and lung weight

Temperature data were retrieved from the implanted temperature loggers and consisted of measurements taken every 30 min. Baseline temperature was calculated as the average temperature in the 5 days before infection. The change in temperature was calculated as deviation from baseline (ΔT). The area under the curve was calculated as the total ΔT up until 5 dpi. Values smaller than "baseline − 2 × SD of baseline" were excluded, as these often occur because of anesthesia. Relative bodyweight and relative lung weight are expressed as a percentage of bodyweight or ratio on the day of infection.

Statistical analysis

All the statistical tests carried out aimed at detecting differences between the distributions of responses in two treatment groups (e.g., H1N1/mRNA and placebo), with each response pertaining to a given stimulus (or measured variable, e.g., body weight) on a given tissue on a given day. The tests are based on the "sum statistic" (*81*) as implemented in the R package "coin" (*82*), in the guise of the function "independence_test," possibly with blocking in the event that some experiments were performed on different days (in which case the data from the same experiment are collected in the same block) and with the (exact) *P* values estimated by random permutations. The tests were grouped into various themes based on tissue and assay (e.g., all stimulations for lung IFN-γ ELISpot), and the Benjamini-Hochberg (BH) method (*83*) was used separately per theme to control the false discovery rate at the level of 10%. Only the results of the tests that passed through the BH method are reported and commented upon in Results. The overall proportion of spurious results (over all the themes) is expected to be at most 10% of all those reported. Tables with the complete results of the tests and multiple testing corrections are available in data file S1. The results reported are illustrated by graphs (e.g., box plots) in the main text or in the Supplementary Materials.

IFN-γ–ELISpot spot counts, viral titers, serum titers, and cell counts were log-transformed for statistical testing. We excluded two data points of the flow cytometry data from the data visualization and analysis. These data points (one in PBMC and one in lung) refer to the percentage IFN-γ^+ within $CD4^+$ T cells and were at least two times higher than the nearest data point. No other data was excluded from analysis. The raw data underlying the figures are presented in data file S2. These data are not corrected (e.g., ELISpot responses are not corrected for medium background) or log-transformed.

Supplementary Materials

This PDF file includes:
Figs. S1 to S9
Tables S1 and S2

Other Supplementary Material for this manuscript includes the following:
Data files S1 and S2

View/request a protocol for this paper from *Bio-protocol*.

REFERENCES AND NOTES

1. A. D. Iuliano, K. M. Roguski, H. H. Chang, D. J. Muscatello, R. Palekar, S. Tempia, C. Cohen, J. M. Gran, D. Schanzer, B. J. Cowling, P. Wu, J. Kyncl, L. W. Ang, M. Park, M. Redlberger-Fritz, H. Yu, L. Espenhain, A. Krishnan, G. Emukule, L. van Asten, S. Pereira da Silva, S. Aungkulanon, U. Buchholz, M. A. Widdowson, J. S. Bresee; Global Seasonal Influenza-associated Mortality Collaborator, Estimates of global seasonal influenza-associated respiratory mortality: A modelling study. *Lancet* **391**, 1285–1300 (2018).
2. J. Paget, P. Spreeuwenberg, V. Charu, R. J. Taylor, A. D. Iuliano, J. Bresee, L. Simonsen, C. Viboud; Global Seasonal Influenza-associated Mortality Collaborator Network and, GLaMOR Collaborating Teams, Global mortality associated with seasonal influenza epidemics: New burden estimates and predictors from the GLaMOR Project. *J. Glob. Health* **9**, 020421 (2019).
3. K. Russell, J. R. Chung, A. S. Monto, E. T. Martin, E. A. Belongia, H. Q. McLean, M. Gaglani, K. Murthy, R. K. Zimmerman, M. P. Nowalk, M. L. Jackson, L. A. Jackson, B. Flannery, Influenza vaccine effectiveness in older adults compared with younger adults over five seasons. *Vaccine* **36**, 1272–1278 (2018).
4. M. T. Osterholm, N. S. Kelley, A. Sommer, E. A. Belongia, Efficacy and effectiveness of influenza vaccines: A systematic review and meta-analysis. *Lancet Infect. Dis.* **12**, 36–44 (2012).
5. J. K. Taubenberger, A. H. Reid, R. M. Lourens, R. Wang, G. Jin, T. G. Fanning, Characterization of the 1918 influenza virus polymerase genes. *Nature* **437**, 889–893 (2005).
6. M. Worobey, G. Z. Han, A. Rambaut, Genesis and pathogenesis of the 1918 pandemic H1N1 influenza A virus. *Proc. Natl. Acad. Sci. U.S.A.* **111**, 8107–8112 (2014).
7. C. Ke, C. K. P. Mok, W. Zhu, H. Zhou, J. He, W. Guan, J. Wu, W. Song, D. Wang, J. Liu, Q. Lin, D. K. W. Chu, L. Yang, N. Zhong, Z. Yang, Y. Shu, J. S. M. Peiris, Human infection with highly pathogenic avian influenza A(H7N9) virus, China. *Emerg. Infect. Dis.* **23**, 1332–1340 (2017).
8. World Health Organization, Disease Outbreak News; Avian Influenza A (H5N1)—nited States of America; www.who.int/emergencies/disease-outbreak-news/item/2022-E000111 [accessed 11-9-2022].

9. OIE, High Pathogenicity Avian Influenza (HPAI)—Situation Report. *The World Organisation for Animal Health* 26, 1–7 (2022); www.oie.int/en/document/high-pathogenicity-avian-influenza-hpai-situation-report-26/.
10. S. Herfst, E. J. Schrauwen, M. Linster, S. Chutinimitkul, E. de Wit, V. J. Munster, E. M. Sorrell, T. M. Bestebroer, D. F. Burke, D. J. Smith, G. F. Rimmelzwaan, A. D. Osterhaus, R. A. Fouchier, Airborne transmission of influenza A/H5N1 virus between ferrets. *Science* **336**, 1534–1541 (2012).
11. M. Linster, S. van Boheemen, M. de Graaf, E. J. A. Schrauwen, P. Lexmond, B. Manz, T. M. Bestebroer, J. Baumann, D. van Riel, G. F. Rimmelzwaan, A. Osterhaus, M. Matrosovich, R. A. M. Fouchier, S. Herfst, Identification, characterization, and natural selection of mutations driving airborne transmission of A/H5N1 virus. *Cell* **157**, 329–339 (2014).
12. M. Imai, T. Watanabe, M. Hatta, S. C. Das, M. Ozawa, K. Shinya, G. Zhong, A. Hanson, H. Katsura, S. Watanabe, C. Li, E. Kawakami, S. Yamada, M. Kiso, Y. Suzuki, E. A. Maher, G. Neumann, Y. Kawaoka, Experimental adaptation of an influenza H5 HA confers respiratory droplet transmission to a reassortant H5 HA/H1N1 virus in ferrets. *Nature* **486**, 420–428 (2012).
13. F. Krammer, P. Palese, Advances in the development of influenza virus vaccines. *Nat. Rev. Drug Discov.* **14**, 167–182 (2015).
14. R. Nachbagauer, P. Palese, Is a universal influenza virus vaccine possible? *Annu. Rev. Med.* **71**, 315–327 (2020).
15. C. E. van de Sandt, J. H. Kreijtz, G. de Mutsert, M. M. Geelhoed-Mieras, M. L. Hillaire, S. E. Vogelzang-van Trierum, A. D. Osterhaus, R. A. Fouchier, G. F. Rimmelzwaan, Human cytotoxic T lymphocytes directed to seasonal influenza A viruses cross-react with the newly emerging H7N9 virus. *J. Virol.* **88**, 1684–1693 (2014).
16. W. Tu, H. Mao, J. Zheng, Y. Liu, S. S. Chiu, G. Qin, P. L. Chan, K. T. Lam, J. Guan, L. Zhang, Y. Guan, K. Y. Yuen, J. S. Peiris, Y. L. Lau, Cytotoxic T lymphocytes established by seasonal human influenza cross-react against 2009 pandemic H1N1 influenza virus. *J. Virol.* **84**, 6527–6535 (2010).
17. E. J. Grant, T. M. Josephs, L. Loh, E. B. Clemens, S. Sant, M. Bharadwaj, W. Chen, J. Rossjohn, S. Gras, K. Kedzierska, Broad CD8$^+$ T cell cross-recognition of distinct influenza A strains in humans. *Nat. Commun.* **9**, 5427 (2018).
18. M. Koutsakos, K. Kedzierska, K. Subbarao, Immune responses to avian influenza viruses. *J. Immunol.* **202**, 382–391 (2019).
19. J. M. Jansen, T. Gerlach, H. Elbahesh, G. F. Rimmelzwaan, G. Saletti, Influenza virus-specific CD4$^+$ and CD8$^+$ T cell-mediated immunity induced by infection and vaccination. *J. Clin. Virol.* **119**, 44–52 (2019).
20. S. Sridhar, S. Begom, A. Bermingham, K. Hoschler, W. Adamson, W. Carman, T. Bean, W. Barclay, J. J. Deeks, A. Lalvani, Cellular immune correlates of protection against symptomatic pandemic influenza. *Nat. Med.* **19**, 1305–1312 (2013).
21. T. M. Wilkinson, C. K. Li, C. S. Chui, A. K. Huang, M. Perkins, J. C. Liebner, R. Lambkin-Williams, A. Gilbert, J. Oxford, B. Nicholas, K. J. Staples, T. Dong, D. C. Douek, A. J. McMichael, X. N. Xu, Preexisting influenza-specific CD4$^+$ T cells correlate with disease protection against influenza challenge in humans. *Nat. Med.* **18**, 274–280 (2012).
22. Z. Wang, Y. Wan, C. Qiu, S. Quinones-Parra, Z. Zhu, L. Loh, D. Tian, Y. Ren, Y. Hu, X. Zhang, P. G. Thomas, M. Inouye, P. C. Doherty, K. Kedzierska, J. Xu, Recovery from severe H7N9 disease is associated with diverse response mechanisms dominated by CD8$^+$ T cells. *Nat. Commun.* **6**, 6833 (2015).
23. R. Bodewes, J. H. Kreijtz, G. van Amerongen, M. L. Hillaire, S. E. Vogelzang-van Trierum, N. J. Nieuwkoop, P. van Run, T. Kuiken, R. A. Fouchier, A. D. Osterhaus, G. F. Rimmelzwaan, Infection of the upper respiratory tract with seasonal influenza A(H3N2) virus induces protective immunity in ferrets against infection with A(H1N1)pdm09 virus after intranasal, but not intratracheal, inoculation. *J. Virol.* **87**, 4293–4301 (2013).
24. K. van de Ven, F. de Heij, H. van Dijken, J. A. Ferreira, J. de Jonge, Systemic and respiratory T-cells induced by seasonal H1N1 influenza protect against pandemic H2N2 in ferrets. *Commun. Biol.* **3**, 564 (2020).
25. K. E. Gooch, A. C. Marriott, K. A. Ryan, P. Yeates, G. S. Slack, P. J. Brown, R. Fothergill, C. J. Whittaker, M. W. Carroll, Heterosubtypic cross-protection correlates with cross-reactive interferon-gamma-secreting lymphocytes in the ferret model of influenza. *Sci. Rep.* **9**, 2617 (2019).
26. R. Bodewes, J. H. Kreijtz, M. M. Geelhoed-Mieras, G. van Amerongen, R. J. Verburgh, S. E. van Trierum, T. Kuiken, R. A. Fouchier, A. D. Osterhaus, G. F. Rimmelzwaan, Vaccination against seasonal influenza A/H3N2 virus reduces the induction of heterosubtypic immunity against influenza A/H5N1 virus infection in ferrets. *J. Virol.* **85**, 2695–2702 (2011).
27. N. Van Braeckel-Budimir, S. M. Varga, V. P. Badovinac, J. T. Harty, Repeated antigen exposure extends the durability of influenza-specific lung-resident memory CD8$^+$ T cells and heterosubtypic immunity. *Cell Rep.* **24**, 3374–3382.e3 (2018).
28. B. Slütter, N. Van Braeckel-Budimir, G. Abboud, S. M. Varga, S. Salek-Ardakani, J. T. Harty, Dynamics of influenza-induced lung-resident memory T cells underlie waning heterosubtypic immunity. *Sci. Immunol.* **2**, eaag2031 (2017).
29. C. S. Eickhoff, F. E. Terry, L. Peng, K. A. Meza, I. G. Sakala, D. Van Aartsen, L. Moise, W. D. Martin, J. Schriewer, R. M. Buller, A. S. De Groot, D. F. Hoft, Highly conserved influenza T cell epitopes induce broadly protective immunity. *Vaccine* **37**, 5371–5381 (2019).
30. T. G. Evans, L. Bussey, E. Eagling-Vose, K. Rutkowski, C. Ellis, C. Argent, P. Griffin, J. Kim, S. Thackwray, S. Shakib, J. Doughty, J. Gillies, J. Wu, J. Druce, M. Pryor, S. Gilbert, Efficacy and safety of a universal influenza A vaccine (MVA-NP+M1) in adults when given after seasonal quadrivalent influenza vaccine immunisation (FLU009): A phase 2b, randomised, double-blind trial. *Lancet Infect. Dis.* **22**, 857–866 (2022).
31. N. Pardi, M. J. Hogan, F. W. Porter, D. Weissman, mRNA vaccines—A new era in vaccinology. *Nat. Rev. Drug Discov.* **17**, 261–279 (2018).
32. F. B. Scorza, N. Pardi, New kids on the block: RNA-based influenza virus vaccines. *Vaccines* **6**, 20 (2018).
33. M. J. Hogan, N. Pardi, mRNA vaccines in the COVID-19 pandemic and beyond. *Annu. Rev. Med.* **73**, 17–39 (2022).
34. V. Oberhardt, H. Luxenburger, J. Kemming, I. Schulien, K. Ciminski, S. Giese, B. Csernalabics, J. Lang-Meli, I. Janowska, J. Staniek, K. Wild, K. Basho, M. S. Marinescu, J. Fuchs, F. Topfstedt, A. Janda, O. Sogukpinar, H. Hilger, K. Stete, F. Emmerich, B. Bengsch, C. F. Waller, S. Rieg, Sagar, T. Boettler, K. Zoldan, G. Kochs, M. Schwemmle, M. Rizzi, R. Thimme, C. Neumann-Haefelin, M. Hofmann, Rapid and stable mobilization of CD8$^+$ T cells by SARS-CoV-2 mRNA vaccine. *Nature* **597**, 268–273 (2021).
35. Z. Wang, F. Schmidt, Y. Weisblum, F. Muecksch, C. O. Barnes, S. Finkin, D. Schaefer-Babajew, M. Cipolla, C. Gaebler, J. A. Lieberman, T. Y. Oliveira, Z. Yang, M. E. Abernathy, K. E. Huey-Tubman, A. Hurley, M. Turroja, K. A. West, K. Gordon, K. G. Millard, V. Ramos, J. Da Silva, J. Xu, R. A. Colbert, R. Patel, J. Dizon, C. Unson-O'Brien, I. Shimeliovich, A. Gazumyan, M. Caskey, P. J. Bjorkman, R. Casellas, T. Hatziioannou, P. D. Bieniasz, M. C. Nussenzweig, mRNA vaccine-elicited antibodies to SARS-CoV-2 and circulating variants. *Nature* **592**, 616–622 (2021).
36. F. Amanat, M. Thapa, T. Lei, S. M. S. Ahmed, D. C. Adelsberg, J. M. Carreno, S. Strohmeier, A. J. Schmitz, S. Zafar, J. Q. Zhou, W. Rijnink, H. Alshammary, N. Borcherding, A. G. Reiche, K. Srivastava, E. M. Sordillo, H. van Bakel, I. Personalized Virology, J. S. Turner, G. Bajic, V. Simon, A. H. Ellebedy, F. Krammer, SARS-CoV-2 mRNA vaccination induces functionally diverse antibodies to NTD, RBD, and S2. *Cell* **184**, 3936–3948.e10 (2021).
37. U. Sahin, A. Muik, E. Derhovanessian, I. Vogler, L. M. Kranz, M. Vormehr, A. Baum, K. Pascal, J. Quandt, D. Maurus, S. Brachtendorf, V. Lorks, J. Sikorski, R. Hilker, D. Becker, A. K. Eller, J. Grutzner, C. Boesler, C. Rosenbaum, M. C. Kuhnle, U. Luxemburger, A. Kemmer-Bruck, D. Langer, M. Bexon, S. Bolte, K. Kariko, T. Palanche, B. Fischer, A. Schultz, P. Y. Shi, C. Fontes-Garfias, J. L. Perez, K. A. Swanson, J. Loschko, I. L. Scully, M. Cutler, W. Kalina, C. A. Kyratsous, D. Cooper, P. R. Dormitzer, K. U. Jansen, O. Tureci, COVID-19 vaccine BNT162b1 elicits human antibody and TH1 T cell responses. *Nature* **586**, 594–599 (2020).
38. A. Zollner, C. Watschinger, A. Rossler, M. R. Farcet, A. Penner, V. Bohm, S. J. Kiechl, G. Stampfel, R. Hintenberger, H. Tilg, R. Koch, M. Antlanger, T. R. Kreil, J. Kimpel, A. R. Moschen, B and T cell response to SARS-CoV-2 vaccination in health care professionals with and without previous COVID-19. *EBioMedicine* **70**, 103539 (2021).
39. N. Pardi, M. J. Hogan, D. Weissman, Recent advances in mRNA vaccine technology. *Curr. Opin. Immunol.* **65**, 14–20 (2020).
40. A. W. Freyn, J. Ramos da Silva, V. C. Rosado, C. M. Bliss, M. Pine, B. L. Mui, Y. K. Tam, T. D. Madden, L. C. de Souza Ferreira, D. Weissman, F. Krammer, L. Coughlan, P. Palese, N. Pardi, R. Nachbagauer, A multi-targeting, nucleoside-modified mRNA influenza virus vaccine provides broad protection in mice. *Mol. Ther.* **28**, 1569–1584 (2020).
41. R. A. Feldman, R. Fuhr, I. Smolenov, A. Mick Ribeiro, L. Panther, M. Watson, J. J. Senn, M. Smith, Almarsson, H. S. Pujar, M. E. Laska, J. Thompson, T. Zaks, G. Ciaramella, mRNA vaccines against H10N8 and H7N9 influenza viruses of pandemic potential are immunogenic and well tolerated in healthy adults in phase 1 randomized clinical trials. *Vaccine* **37**, 3326–3334 (2019).
42. K. Bahl, J. J. Senn, O. Yuzhakov, A. Bulychev, L. A. Brito, K. J. Hassett, M. E. Laska, M. Smith, O. Almarsson, J. Thompson, A. M. Ribeiro, M. Watson, T. Zaks, G. Ciaramella, Preclinical and clinical demonstration of immunogenicity by mRNA vaccines against H10N8 and H7N9 influenza viruses. *Mol. Ther.* **25**, 1316–1327 (2017).
43. X. Zhuang, Y. Qi, M. Wang, N. Yu, F. Nan, H. Zhang, M. Tian, C. Li, H. Lu, N. Jin, mRNA vaccines encoding the HA protein of influenza A H1N1 virus delivered by cationic lipid nanoparticles induce protective immune responses in mice. *Vaccines* **8**, 123 (2020).
44. N. Pardi, J. M. Carreño, G. O'Dell, J. Tan, C. Bajusz, H. Muramatsu, W. Rijnink, S. Strohmeier, M. Loganathan, D. Bielak, M. M. H. Sung, Y. K. Tam, F. Krammer, M. McMahon, Development of a pentavalent broadly protective nucleoside-modified mRNA vaccine against influenza B viruses. *Nat. Commun.* **13**, 4677 (2022).
45. A. C. Hayward, L. Wang, N. Goonetilleke, E. B. Fragaszy, A. Bermingham, A. Copas, O. Dukes, E. R. C. Millett, I. Nazareth, J. S. Nguyen-Van-Tam, J. M. Watson, M. Zambon, A. M. Johnson, A. J. McMichael, Natural T cell-mediated protection against seasonal and pandemic influenza: Results of the flu watch cohort study. *Am. J. Respir. Crit. Care Med.* **191**, 1422–1431 (2015).

46. N. Pardi, S. Tuyishime, H. Muramatsu, K. Kariko, B. L. Mui, Y. K. Tam, T. D. Madden, M. J. Hope, D. Weissman, Expression kinetics of nucleoside-modified mRNA delivered in lipid nanoparticles to mice by various routes. *J. Control. Release* **217**, 345–351 (2015).
47. A. Pizzolla, T. H. O. Nguyen, J. M. Smith, A. G. Brooks, K. Kedzieska, W. R. Heath, P. C. Reading, L. M. Wakim, Resident memory CD8$^+$ T cells in the upper respiratory tract prevent pulmonary influenza virus infection. *Sci. Immunol.* **2**, eaam6970 (2017).
48. H. D. Chang, A. Radbruch, Maintenance of quiescent immune memory in the bone marrow. *Eur. J. Immunol.* **51**, 1592–1601 (2021).
49. E. Dolgin, mRNA flu shots move into trials. *Nat. Rev. Drug Discov.* **20**, 801–803 (2021).
50. S. Su, M. Gu, D. Liu, J. Cui, G. F. Gao, J. Zhou, X. Liu, Epidemiology, evolution, and pathogenesis of H7N9 influenza viruses in five epidemic waves since 2013 in China. *Trends Microbiol.* **25**, 713–728 (2017).
51. T. Wu, Y. Hu, Y. T. Lee, K. R. Bouchard, A. Benechet, K. Khanna, L. S. Cauley, Lung-resident memory CD8 T cells (TRM) are indispensable for optimal cross-protection against pulmonary virus infection. *J. Leukoc. Biol.* **95**, 215–224 (2014).
52. K. D. Zens, J. K. Chen, D. L. Farber, Vaccine-generated lung tissue–resident memory T cells provide heterosubtypic protection to influenza infection. *JCI Insight* **1**, e85832 (2016).
53. D. Laczko, M. J. Hogan, S. A. Toulmin, P. Hicks, K. Lederer, B. T. Gaudette, D. Castano, F. Amanat, H. Muramatsu, T. H. Oguin III, A. Ojha, L. Zhang, Z. Mu, R. Parks, T. B. Manzoni, B. Roper, S. Strohmeier, I. Tombacz, L. Arwood, R. Nachbagauer, K. Kariko, J. Greenhouse, L. Pessaint, M. Porto, T. Putman-Taylor, A. Strasbaugh, T. A. Campbell, P. J. C. Lin, Y. K. Tam, G. D. Sempowski, M. Farzan, H. Choe, K. O. Saunders, B. F. Haynes, H. Andersen, L. C. Eisenlohr, D. Weissman, F. Krammer, P. Bates, D. Allman, M. Locci, N. Pardi, A single immunization with nucleoside-modified mRNA vaccines elicits strong cellular and humoral immune responses against SARS-CoV-2 in mice. *Immunity* **53**, 724–732.e7 (2020).
54. M. Li, M. Zhao, Y. Fu, Y. Li, T. Gong, Z. Zhang, X. Sun, Enhanced intranasal delivery of mRNA vaccine by overcoming the nasal epithelial barrier via intra- and paracellular pathways. *J. Control. Release* **228**, 9–19 (2016).
55. M. Feuerer, P. Beckhove, N. Garbi, Y. Mahnke, A. Limmer, M. Hommel, G. J. Hammerling, B. Kyewski, A. Hamann, V. Umansky, V. Schirrmacher, Bone marrow as a priming site for T-cell responses to blood-borne antigen. *Nat. Med.* **9**, 1151–1157 (2003).
56. D. Duffy, H. Perrin, V. Abadie, N. Benhabiles, A. Boissonnas, C. Liard, B. Descours, D. Reboulleau, O. Bonduelle, B. Verrier, N. Van Rooijen, C. Combadiere, B. Combadiere, Neutrophils transport antigen from the dermis to the bone marrow, initiating a source of memory CD8$^+$ T cells. *Immunity* **37**, 917–929 (2012).
57. F. Di Rosa, R. Pabst, The bone marrow: A nest for migratory memory T cells. *Trends Immunol.* **26**, 360–366 (2005).
58. M. F. Pascutti, S. Geerman, N. Collins, G. Brasser, B. Nota, R. Stark, F. Behr, A. Oja, E. Slot, E. Panagioti, J. E. Prier, S. Hickson, M. C. Wolkers, M. H. M. Heemskerk, P. Hombrink, R. Arens, L. K. Mackay, K. van Gisbergen, M. A. Nolte, Peripheral and systemic antigens elicit an expandable pool of resident memory CD8$^+$ T cells in the bone marrow. *Eur. J. Immunol.* **49**, 853–872 (2019).
59. P. Naaber, L. Tserel, K. Kangro, E. Sepp, V. Jurjenson, A. Adamson, L. Haljasmagi, A. P. Rumm, R. Maruste, J. Karner, J. M. Gerhold, A. Planken, M. Ustav, K. Kisand, P. Peterson, Dynamics of antibody response to BNT162b2 vaccine after six months: A longitudinal prospective study. *Lancet Reg. Health Eur.* **10**, 100208 (2021).
60. V. Naranbhai, W. F. Garcia-Beltran, C. C. Chang, C. B. Mairena, J. C. Thierauf, G. Kirkpatrick, M. L. Onozato, J. Cheng, K. J. St Denis, E. C. Lam, C. Kaseke, R. Tano-Menka, D. Yang, M. Pavlovic, W. Yang, A. Kui, T. E. Miller, M. G. Astudillo, J. E. Cahill, A. S. Dighe, D. J. Gregory, M. C. Poznansky, G. D. Gaiha, A. B. Balazs, A. J. Iafrate, Comparative immunogenicity and effectiveness of mRNA-1273, BNT162b2 and Ad26.COV2.S COVID-19 vaccines. *J Infect Dis* **225**, 1141–1150 (2021).
61. D. M. Carragher, D. A. Kaminski, A. Moquin, L. Hartson, T. D. Randall, A novel role for non-neutralizing antibodies against nucleoprotein in facilitating resistance to influenza virus. *J. Immunol.* **181**, 4168–4176 (2008).
62. M. W. LaMere, H. T. Lam, A. Moquin, L. Haynes, F. E. Lund, T. D. Randall, D. A. Kaminski, Contributions of antinucleoprotein IgG to heterosubtypic immunity against influenza virus. *J. Immunol.* **186**, 4331–4339 (2011).
63. S. Jegaskanda, M. D. T. Co, J. Cruz, K. Subbarao, F. A. Ennis, M. Terajima, Induction of H7N9-cross-reactive antibody-dependent cellular cytotoxicity antibodies by human seasonal influenza A viruses that are directed toward the nucleoprotein. *J Infect Dis* **215**, 818–823 (2017).
64. H. A. Vanderven, F. Ana-Sosa-Batiz, S. Jegaskanda, S. Rockman, K. Laurie, I. Barr, W. Chen, B. Wines, P. M. Hogarth, T. Lambe, S. C. Gilbert, M. S. Parsons, S. J. Kent, What lies beneath: Antibody dependent natural killer cell activation by antibodies to internal influenza virus proteins. *EBioMedicine* **8**, 277–290 (2016).
65. D. Y. Oh, A. C. Hurt, Using the ferret as an animal model for investigating influenza antiviral effectiveness. *Front. Microbiol.* **7**, 80 (2016).
66. F. P. Polack, S. J. Thomas, N. Kitchin, J. Absalon, A. Gurtman, S. Lockhart, J. L. Perez, G. Perez Marc, E. D. Moreira, C. Zerbini, R. Bailey, K. A. Swanson, S. Roychoudhury, K. Koury, P. Li, W. V. Kalina, D. Cooper, R. W. Frenck Jr., L. L. Hammitt, O. Tureci, H. Nell, A. Schaefer, S. Unal, D. B. Tresnan, S. Mather, P. R. Dormitzer, U. Sahin, K. U. Jansen, W. C. Gruber; C4591001 Clinical Trial Group, Safety and efficacy of the BNT162b2 mRNA COVID-19 vaccine. *N. Engl. J. Med.* **383**, 2603–2615 (2020).
67. L. R. Baden, H. M. El Sahly, B. Essink, K. Kotloff, S. Frey, R. Novak, D. Diemert, S. A. Spector, N. Rouphael, C. B. Creech, J. McGettigan, S. Khetan, N. Segall, J. Solis, A. Brosz, C. Fierro, H. Schwartz, K. Neuzil, L. Corey, P. Gilbert, H. Janes, D. Follmann, M. Marovich, J. Mascola, L. Polakowski, J. Ledgerwood, B. S. Graham, H. Bennett, R. Pajon, C. Knightly, B. Leav, W. Deng, H. Zhou, S. Han, M. Ivarsson, J. Miller, T. Zaks, COVE Study Group, Efficacy and safety of the mRNA-1273 SARS-CoV-2 vaccine. *N. Engl. J. Med.* **384**, 403–416 (2021).
68. J. Smetana, R. Chlibek, J. Shaw, M. Splino, R. Prymula, Influenza vaccination in the elderly. *Hum. Vaccin. Immunother.* **14**, 540–549 (2018).
69. Moderna, Moderna's Respiratory Vaccines: Flu vaccines (mRNA-1010/−11/−12/−20/−30); https://s29.q4cdn.com/435878511/files/doc_downloads/program_detail/respiratory/Flu-(05-04-22).pdf [accessed 4 May 2022].
70. BiondVax Pharmaceuticals, A Pivotal Trial to Assess the Safety and Clinical Efficacy of the M-001 as a Standalone Universal Flu Vaccine; https://clinicaltrials.gov/ct2/show/study/NCT03450915 [accessed 19 August 2022].
71. R. R. Goel, M. M. Painter, S. A. Apostolidis, D. Mathew, W. Meng, A. M. Rosenfeld, K. A. Lundgreen, A. Reynaldi, D. S. Khoury, A. Pattekar, S. Gouma, L. Kuri-Cervantes, P. Hicks, S. Dysinger, A. Hicks, H. Sharma, S. Herring, S. Korte, A. E. Baxter, D. A. Oldridge, J. R. Giles, M. E. Weirick, C. M. McAllister, M. Awofolaju, N. Tanenbaum, E. M. Drapeau, J. Dougherty, S. Long, K. D'Andrea, J. T. Hamilton, M. McLaughlin, J. C. Williams, S. Adamski, O. Kuthuru; UPenn COVID Processing Unit, I. Frank, M. R. Betts, L. A. Vella, A. Grifoni, D. Weiskopf, A. Sette, S. E. Hensley, M. P. Davenport, P. Bates, E. T. L. Prak, A. R. Greenplate, E. J. Wherry, mRNA vaccines induce durable immune memory to SARS-CoV-2 and variants of concern. *Science* **374**, abm0829 (2021).
72. S. A. Valkenburg, L. L. M. Poon, Universal influenza vaccines are futile when benchmarked against seasonal influenza vaccines. *Lancet Infect. Dis.* **22**, 750–751 (2022).
73. A. W. Freyn, M. Pine, V. C. Rosado, M. Benz, H. Muramatsu, M. Beattie, Y. K. Tam, F. Krammer, P. Palese, R. Nachbagauer, M. McMahon, N. Pardi, Antigen modifications improve nucleoside-modified mRNA-based influenza virus vaccines in mice. *Mol. Ther. Methods Clin. Dev.* **22**, 84–95 (2021).
74. M. Baiersdorfer, G. Boros, H. Muramatsu, A. Mahiny, I. Vlatkovic, U. Sahin, K. Kariko, A facile method for the removal of dsRNA contaminant from in vitro-transcribed mRNA. *Mol. Ther. Nucleic Acids* **15**, 26–35 (2019).
75. K. van de Ven, H. van Dijken, L. Wijsman, A. Gomersbach, T. Schouten, J. Kool, S. Lenz, P. Roholl, A. Meijer, P. B. van Kasteren, J. de Jonge, Pathology and immunity after SARS-CoV-2 infection in male ferrets is affected by age and inoculation route. *Front. Immunol.* **12**, 750229 (2021).
76. R Core Team. (R Foundation for Statistical Computing, 2021).
77. World Health Organization, *Manual for the laboratory diagnosis and virological surveillance of influenza* (World Health Organization, Geneva, 2011), chap. xii, 140 pp.
78. J. de Jonge, H. van Dijken, F. de Heij, S. Spijkers, J. Mouthaan, R. de Jong, P. Roholl, E. A. Adami, M. A. Akamatsu, P. L. Ho, L. Brunner, N. Collin, M. Friede, J. A. Ferreira, W. Luytjes, H7N9 influenza split vaccine with SWE oil-in-water adjuvant greatly enhances cross-reactive humoral immunity and protection against severe pneumonia in ferrets. *NPJ Vaccines* **5**, 38 (2020).
79. L. J. Reed, H. Muench, A simple method of estimating fifty per cent endpoints. *Am. J. Hygiene* **27**, 493–497 (1938).
80. J. M. van den Brand, J. H. Kreijtz, R. Bodewes, K. J. Stittelaar, G. van Amerongen, T. Kuiken, J. Simon, R. A. Fouchier, G. Del Giudice, R. Rappuoli, G. F. Rimmelzwaan, A. D. Osterhaus, Efficacy of vaccination with different combinations of MF59-adjuvanted and nonadjuvanted seasonal and pandemic influenza vaccines against pandemic H1N1 (2009) influenza virus infection in ferrets. *J. Virol.* **85**, 2851–2858 (2011).
81. P. R. Rosenbaum, *Observational Studies* (Springer Series in Statistics, 2002).
82. T. Hothorn, K. Hornik, M. A. Wiel, A. Zeileis, Implementing a class of permutation tests: ThecoinPackage. *J. Stat. Softw.* **28**, 1–23 (2008).
83. Y. Benjamini, Y. Hochberg, Controlling the false discovery rate: A practical and powerful approach to multiple testing. *J. R. Stat. Soc. B. Methodol.* **57**, 289–300 (1995).
84. J. de Jonge, I. Isakova-Sivak, H. van Dijken, S. Spijkers, J. Mouthaan, R. de Jong, T. Smolonogina, P. Roholl, L. Rudenko, H7N9 live attenuated influenza vaccine is highly immunogenic, prevents virus replication, and protects against severe bronchopneumonia in ferrets. *Mol. Ther.* **24**, 991–1002 (2016).

Acknowledgments: We would like to thank M. Hendriks, J. Kool, H. P. Guimarães, N. Smits, R. Jacobi, and M. Vos for help during the animal sections; the biotechnicians from the animal facility for excellent care of the animals; and T. Guichelaar and W. Luytjes for critical review of the

manuscript. **Funding:** This work was supported by the Dutch Ministry of Health, Welfare, and Sports (VWS) (to J.d.J. and K.v.d.V.) and NIH grants R01-AI146101 and R01AI153064 (to N.P.).
Author contributions: Conceptualization: K.v.d.V., D.v.B., N.P., and J.d.J. Methodology: K.v.d.V. and J.d.J. Software: J.A.F. Formal analysis: K.v.d.V. and J.v.d.B. Investigation: K.v.d.V., J.L., H.v.D., C.V.B.d.M., S.L., and F.P. Resources: N.P., H.M., M.B.B., and P.J.C.L. Data curation: K.v.d.V. Writing (original draft): K.v.d.V. and J.A.F. Writing (review and editing): J.L., D.v.B., N.P., and J.d.J. Visualization: K.v.d.V. Supervision: J.d.J. Project administration: J.d.J. Funding acquisition: J.d.J. and N.P. **Competing interests:** N.P. is named on a patent describing the use of modified mRNA in LNPs as a vaccine platform. In addition, N.P. is named on a patent filed on universal influenza vaccines using nucleoside-modified mRNA. N.P. has disclosed those interests fully to the University of Pennsylvania and has in place an approved plan for managing any potential conflicts arising from licensing of these patents. M.B.B. and P.J.C.L. are employees of Acuitas Therapeutics. The authors declare that they have no other competing interests. **Data and materials availability:** The statistical analysis underlying the manuscript is available in data file S1. The data underlying the main findings are presented in data file S2. The mRNA vaccines can be provided by the University of Pennsylvania after scientific review and a completed material transfer agreement. Requests for the mRNA vaccines should be submitted to pnorbert@pennmedicine.upenn.edu. All data needed to evaluate the conclusions in the paper are present in the paper and/or the Supplementary Materials.

Submitted 13 May 2022
Accepted 4 November 2022
Published 14 December 2022
10.1126/sciadv.adc9937